Hypertension
JOURNAL OF THE AMERICAN HEART ASSOCIATION

Adenoassociated Virus Mediated Prostacyclin Synthase Expression Prevents Pulmonary Arterial Hypertension in Rats

Takayuki Ito, Takashi Okada, Jun Mimuro, Hiroshi Miyashita, Ryosuke Uchibori, Masashi Urabe, Hiroaki Mizukami, Akihiro Kume, Masafumi Takahashi, Uichi Ikeda, Yoichi Sakata, Kazuyuki Shimada and Keiya Ozawa

Hypertension 2007;50;531-536; originally published online Jul 16, 2007;
DOI: 10.1161/HYPERTENSIONAHA.107.091348
Hypertension is published by the American Heart Association. 7272 Greenville Avenue, Dallas, TX 72514
 Print ISSN: 0194-911X. Online ISSN: 1524-4563

Adenoassociated Virus–Mediated Prostacyclin Synthase Expression Prevents Pulmonary Arterial Hypertension in Rats

Takayuki Ito, Takashi Okada, Jun Mimuro, Hiroshi Miyashita, Ryosuke Uchibori, Masashi Urabe, Hiroaki Mizukami, Akihiro Kume, Masafumi Takahashi, Uichi Ikeda, Yoichi Sakata, Kazuyuki Shimada, Keiya Ozawa

Abstract—Prostacyclin synthase (PGIS) is the final committed enzyme in the metabolic pathway of prostacyclin production. The therapeutic option of intravenous prostacyclin infusion in patients with pulmonary arterial hypertension is limited by the short half-life of the drug and life-threatening catheter-related complications. To develop a better delivery system for prostacyclin, we examined the feasibility of intramuscular injection of an adenoassociated virus (AAV) vector expressing PGIS for preventing monocrotaline-induced pulmonary arterial hypertension in rats. We developed an AAV serotype 1–based vector carrying a human PGIS gene (AAV-PGIS). AAV-PGIS or the control AAV vector expressing enhanced green fluorescent protein was injected into the anterior tibial muscles of 3-week–old male Wistar rats; this was followed by the monocrotaline administration at 7 weeks. Eight weeks after injecting the vector, the plasma levels of 6-keto-prostaglandin $F_{1\alpha}$ increased in a vector dose-dependent manner. At this time point, the PGIS transduction (1×10^{10} genome copies per body) significantly decreased mean pulmonary arterial pressure (33.9 ± 2.4 versus 46.1 ± 3.0 mm Hg; $P<0.05$), pulmonary vascular resistance (0.26 ± 0.03 versus 0.41 ± 0.03 mm Hg $\cdot$ mL^{-1} $\cdot$ min^{-1} $\cdot$ kg^{-1}; $P<0.05$), and medial thickness of the peripheral pulmonary artery ($14.6\pm1.5\%$ versus $23.5\pm0.5\%$; $P<0.01$) as compared with the controls. Furthermore, the PGIS-transduced rats demonstrated significantly improved survival rates as compared with the controls (100% versus 50%; $P<0.05$) at 8 weeks postmonocrotaline administration. An intramuscular injection of AAV-PGIS prevents monocrotaline-pulmonary arterial hypertension in rats and provides a new therapeutic alternative for preventing pulmonary arterial hypertension in humans. (***Hypertension.* 2007;50:531-536.**)

Key Words: hypertension ■ pulmonary ■ gene therapy ■ remodeling ■ prostacyclin synthase

Pulmonary arterial hypertension (PAH) is an intractable disease that leads to increased pulmonary arterial pressure, progressive right heart failure, and premature death; however, no satisfactory treatment has been established for PAH.[1] Although intravenous prostacyclin (PGI_2) therapy prolongs survival in patients with PAH, the use of this treatment option is limited by the short half-life of the drug, requirement for a continuous infusion system, and catheter-related complications.[1,2] PGI_2 synthase (PGIS) is the final committed enzyme in the metabolic pathway of PGI_2 production. PGIS gene transfer is a promising approach for the stable production of endogenous PGI_2.[3–6] However, previous strategies have several limitations both in the selection of delivery routes and in the efficiency of gene expression. For instance, intratracheal gene transfer may deteriorate respiratory function in critically ill subjects, and the intrahepatic approach may cause peritonitis as a result of direct liver puncture. Although an intramuscular approach seems to be safer than the previous approaches, the conventional plasmid-based strategies achieved only transient gene expression and required repeated gene transfer to inhibit pathological remodeling of the pulmonary artery (PA).[6]

In this study, we used an adenoassociated virus (AAV) vector together with an intramuscular approach to obtain more efficient PGI_2 expression. AAV vectors permit efficient and sustained gene expression in nondividing skeletal muscle cells with minimal inflammatory and immune responses. We reported previously that a stable serum concentration of a secretory protein was achieved over a 1-year period by using a single intramuscular injection of several AAV vector (AAV2 and AAV5) serotypes in mice.[7] Currently, AAV1 is one of the most efficient serotypes for muscle transduction.[8,9]

Received March 25, 2007; first decision April 13, 2007; revision accepted June 22, 2007.

From the Divisions of Genetic Therapeutics (T.I., R.U., M.U., H.M., A.K., K.O.), Cardiovascular Medicine (T.I., H.M., K.S.), and Cell and Molecular Medicine (J.M., Y.S.), Jichi Medical University, Tochigi, Japan; the Department of Molecular Therapy (T.O.), National Institute of Neuroscience, National Center of Neurology and Psychiatry, Tokyo, Japan; and the Department of Organ Regeneration (M.T., U.I.), Shinshu University Graduate School of Medicine, Matsumoto, Japan.

Correspondence to Takayuki Ito or Keiya Ozawa, Division of Genetic Therapeutics, Jichi Medical University, 3311-1 Yakushiji, Shimotsuke, Tochigi 329-0498, Japan. E-mail titou@jichi.ac.jp or kozawa@jichi.ac.jp

Hypertension is available at http://hyper.ahajournals.org DOI: 10.1161/HYPERTENSIONAHA.107.091348

Single subcutaneous injection of a pyrrolizidine alkaloid, namely, monocrotaline (MCT), produces severe PAH and PA remodeling in rats. We examined the effects of sustained PGIS expression in preventing PAH development and progression by means of this widely used model and an AAV1 vector.

Methods

Western Blot Analysis for PGIS Expression In Vitro

Human embryonic kidney 293 (HEK293) cells were incubated in 10-cm dishes containing DMEM and nutrient mixture F12 (Invitrogen) with 2% FCS in an atmosphere of 5% CO_2 in air at 37°C. The cells at 70% confluence were transfected with an AAV proviral plasmid encoding human PGIS (phPGIS, a kind gift from Dr Mimuro) or plasmid encoding enhanced green fluorescent protein (eGFP) by using a calcium phosphate method. The cells were harvested 72 hours after transfection, and cell lysates were prepared with a lysis buffer (10 mmol/L of Tris-HCl, 150 mmol/L of NaCl, and 1% NP40 [pH 7.6]) containing Complete Mini protease inhibitor (Roche Diagnostics). For Western blot analysis, 10 μg of the lysate was subjected to 10% SDS-PAGE and transferred to a nitrocellulose membrane. The membrane was blocked and incubated with a 1:500 dilution of rabbit anti-human PGIS polyclonal antibody (a gift from Dr Mimuro) and a 1:5000 dilution of peroxidase-linked anti-rabbit IgG antibody (Amersham Pharmacia Biotech), and immunoreactive bands were visualized using an enhanced chemiluminescence Western blotting kit (Amersham).

AAV-PGIS Production and PGI_2 Expression

We developed a recombinant AAV1-based vector containing the human PGIS or eGFP gene controlled by a modified chicken β-actin promoter with a cytomegalovirus immediate-early enhancer (AAV-PGIS or AAV-eGFP) to obtain efficient transgene expression in skeletal muscle cells. The AAV vectors were prepared according to the previously described 3-plasmid transfection adenovirus-free protocol with minor modifications for enabling the use of an active gassing system.[10,11] In brief, 60% confluent HEK293 cells that were incubated in a large culture vessel with active air circulation were cotransfected with phPGIS, AAV-1 chimeric helper plasmid (p1RepCap), and adenoviral helper plasmid pAdeno (Avigen Inc). The crude viral lysate was purified with 2 rounds of cesium chloride 2-tier centrifugation.[12] The titer of the viral stock was determined against plasmid standards by real-time PCR with primers 5′-CCCGCGAGGTTGTGGTGGAC-3′ and 5′-ATGGGCGGATGCGGTAGC-3′; subsequently, the stock was dissolved in a buffer (50 mmol/L of HEPES [pH 7.4] and 0.15 mol/L of NaCl [HN buffer]) before infection. The HEK293 cells cultured in 6-well plates containing DMEM and nutrient mixture F12 with 5% FCS were infected with AAV-PGIS at 1×10^4 genome copies per cell to evaluate PGI_2 expression in vitro, and the supernatant was harvested after 72 hours. Concentrations of 6-keto-prostaglandin $F_{1\alpha}$ (6-keto-$PGF_{1\alpha}$) in plasma or culture media were determined by enzyme immunoassay (R&D Systems) according to the manufacturer's instructions. The minimum detectable dose of the assay was <1.4 pg/mL. Interassay and intra-assay precision of the kit was <10%.

Animal Models

All of the animal experiments were approved by the Jichi Medical University ethics committee and were performed in accordance with the National Institutes of Health Guide for the Care and Use of Laboratory Animals. To evaluate the efficiency of gene expression in vivo, AAV-eGFP (200 μL; 1×10^{11} gene copies per body) or AAV-PGIS (200 μL; 1×10^{10} to 1×10^{11} gene copies per body) was injected into the bilateral anterior tibial muscles (n=3 each) of 3-week-old male Wistar rats (Clea Japan Inc) weighing 45 to 55 g. For hemodynamics and histological analyses, the rats were divided into 4 groups: sham rats that were administered the HN buffer (group 1, negative control [NC] group; n=4); MCT-PAH rats administered the HN buffer (group 2, MCT group; n=6); MCT rats administered AAV-eGFP (group 3, MCT+eGFP group; n=6); and MCT rats administered AAV-PGIS (group 4, MCT+PGIS group; n=10). After the anesthesia with spontaneous inhalation of 1% isoflurane, the rats in groups 3 and 4 were intramuscularly injected with AAV-eGFP or AAV-PGIS (1×10^{10} gene copies per body), whereas those in groups 1 and 2 were injected with the HN buffer (200 μL). MCT (Wako Pure Chemicals) was dissolved in 0.1 N HCl, and the pH was adjusted to 7.4 with 1.0 N NaOH. After the anesthesia with spontaneous inhalation of 1% isoflurane, all of the rats except for those in the NC group were injected subcutaneously with MCT (40 mg/kg) 4 weeks after the injecting the vector. Blood samples were collected from the tail vein on ethylenediamine tetraacetic acid tubes, and the concentrations of the leukocytes, platelets, hematocrit, alanine aminotransferase, and creatinine were determined by standard procedures.

Hemodynamics Analysis

Four weeks after the MCT injection, the rats were anesthetized with spontaneous inhalation of 1% isoflurane, and a tracheotomy was performed. Then, they were mechanically ventilated with 1% isoflurane (tidal volume, 10 mL/kg; respiratory rate, 30 breaths per minute) through a tracheostomy. After the thoracic cavity was opened using a midsternal approach, 2F high-fidelity manometer-tipped catheters (SPC-320; Millar Instruments Inc) were inserted directly into the right or left ventricle, and an ultrasonic flow probe (flow probe 2.5S176; Transonic Systems Inc) was placed on the ascending root of the aorta. The heart rate, mean pulmonary arterial pressure (mPAP), aortic systolic arterial pressure, left ventricular end-diastolic pressure (LVEDP), and mean aortic flow indicating the cardiac output (CO) were measured. Cardiac indices (CI) and pulmonary vascular resistance (PVR) were calculated using the following formula: CI ($mL\cdot min^{-1}\cdot kg^{-1}$)=CO/body weight, PVR ($mm\,Hg\cdot mL^{-1}\cdot min^{-1}\cdot kg^{-1}$)=(mPAP−LVEDP)/CI.

Ventricular Weight Measurement and Morphometric Analysis of the PA

After the hemodynamic analysis, the rats were killed with an overdose (5%) of isoflurane through a tracheostomy. Their lungs were perfused with 5 mL of saline followed by 10 mL of cold 4% paraformaldehyde. Each ventricle and the lungs were then excised, dissected free, and weighed. The weight ratio of the right ventricle to the left ventricle plus septum [RV/(LV+S)] was calculated as an index of right ventricular hypertrophy (RVH). The lung tissues were fixed overnight at 4°C in 4% paraformaldehyde and frozen in Tissue-Tek OCT compound (Sakura Finetechnical Co) at −20°C. Hematoxylin and eosin staining was performed on 7-μm–thick sections that were subsequently examined using light microscopy. A morphometric analysis was performed on a PA having an external diameter of 25 to 50 μm or 51 to 100 μm. The medial wall thickness was calculated using the following formula: medial thickness (%)=medial wall thickness/external diameter×100.[13] For the quantitative analysis, 30 vessels of each rat were measured and averaged randomly by the 2 external observers.

Survival Analysis

The 3-week-old Wistar rats were divided into 3 groups (MCT, MCT+eGFP, and MCT+PGIS; n=8 each). After the anesthesia with spontaneous inhalation of 1% isoflurane, the rats in the MCT+eGFP or MCT+PGIS group were intramuscularly injected with AAV-eGFP or AAV-PGIS at 1×10^{10} genome copies per body, respectively. Under the same anesthetic condition, all of the rats were injected subcutaneously with MCT (40 mg/kg) at 4 weeks after injecting the vector. The survival rate was estimated from the date of the MCT administration until death or after 8 weeks of the injection. Survival curves were analyzed using the Kaplan-Meier method and compared by log-rank tests.

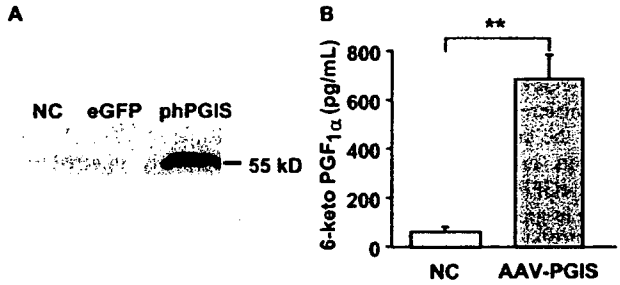

Figure 1. Expression of PGIS and PGI_2 in vitro. A, Western blot analysis of PGIS expression in HEK293 cells after plasmid transfection. The cells were harvested 72 hours after transfection with phPGIS or eGFP. B, AAV vector-mediated PGI_2 expression in HEK293 cells. The PGI_2 levels were estimated by measuring the amount of 6-keto-$PGF_{1\alpha}$, a stable metabolite of PGI_2, in the culture supernatant by enzyme immunoassay 72 hours after infecting the cells (n=4 each) with AAV-PGIS (1×10^4 genome copies per cell). Data are presented as mean±SEM. **$P<0.01$. NC indicates untreated negative control.

Statistical Analysis

The statistical analysis and correlations were performed using StatView (Abacus Concepts, Inc). Data are presented as mean±SEM. Differences in parameters were evaluated using ANOVA combined with Fisher's test. A value of $P<0.05$ was considered statistically significant.

Results

Expression of PGIS and PGI_2 In Vitro

Western blot analysis revealed that transfection of the HEK293 cells with phPGIS but not with a plasmid carrying the eGFP gene enhanced the production of the PGIS protein (Figure 1A). Infection of the cells with AAV-PGIS at 1×10^4 genome copies per cell significantly increased the concentration of 6-keto-$PGF_{1\alpha}$, a stable metabolite of PGI_2, in culture supernatants as compared with that without vector infection (Figure 1B).

AAV Vector-Mediated Systemic PGI_2 Expression in the Rats

Four weeks after the injection of AAV vectors (1×10^{10} genome copies per body), the PGIS-transduced rats began exhibiting significant increases in the plasma 6-keto-$PGF_{1\alpha}$ levels as compared with the control rats (Figure 2A). Eight weeks after the injection, the 6-keto-$PGF_{1\alpha}$ levels increased further in a vector dose-dependent manner in the treated rats (Figure 2B) as compared with the untreated controls (6.68±1.33 versus 1.62±0.30 ng/mL, 1×10^{11} versus 1×10^{10} genome copies per body, respectively; $P<0.05$; n=3 each). The vectors at 1×10^{10} genome copies per body were used for all of the subsequent experiments. In contrast, injection of 1×10^{11} genome copies per body of AAV-eGFP produced no significant change in the 6-keto-$PGF_{1\alpha}$ levels.

Effects of PGI_2 Expression on Hemodynamics and RVH

Four weeks after the MCT administration, the mPAP levels were significantly elevated in the treated rats as compared with the untreated controls (Figure 3A). Treatment with AAV-PGIS but not AAV-eGFP significantly inhibited this increase (Figure 3A). In addition, the expression of PGI_2

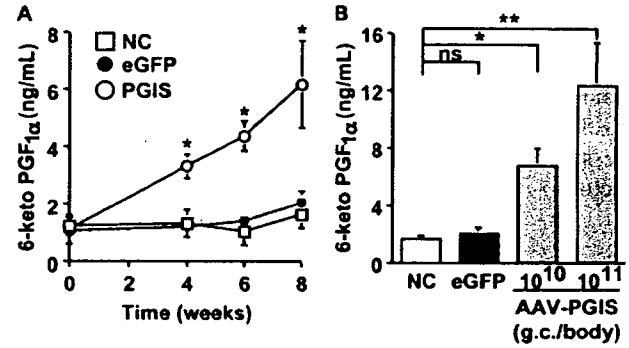

Figure 2. AAV vector-mediated systemic expression of PGI_2 in vivo. The concentration of plasma 6-keto-$PGF_{1\alpha}$ was determined by enzyme immunoassay after a single injection of AAV-PGIS into the anterior tibial muscle of 3-week-old male Wistar rats. A, Time course of plasma 6-keto-$PGF_{1\alpha}$ levels after injection of AAV-PGIS at 1×10^{10} genome copies per body. B, Vector dose dependency of plasma 6-keto-$PGF_{1\alpha}$ levels 8 weeks after the injection. The rats injected with AAV-eGFP (1×10^{11} genome copies per body) were used as controls. Data are presented as mean±SEM (n=3 animals per group). ns indicates not statistically significant; NC, untreated negative control. *$P<0.05$ vs NC; **$P<0.01$.

significantly mitigated an increase in PVR and a decrease in CI that were induced by MCT (Figure 3B and 3C, respectively); however, it produced no significant changes in the heart rate and aortic systolic arterial pressure (Table). PGI_2 expression also had a beneficial effect on RVH. Treatment with AAV-PGIS but not AAV-eGFP significantly inhibited the MCT-induced increase in RV/(LV+S) (Figure 3D).

Effects on Medial Hypertrophy of the PA

Medial hypertrophy is a hallmark of pathological vascular remodeling in PAH. Four weeks after the MCT injection, the

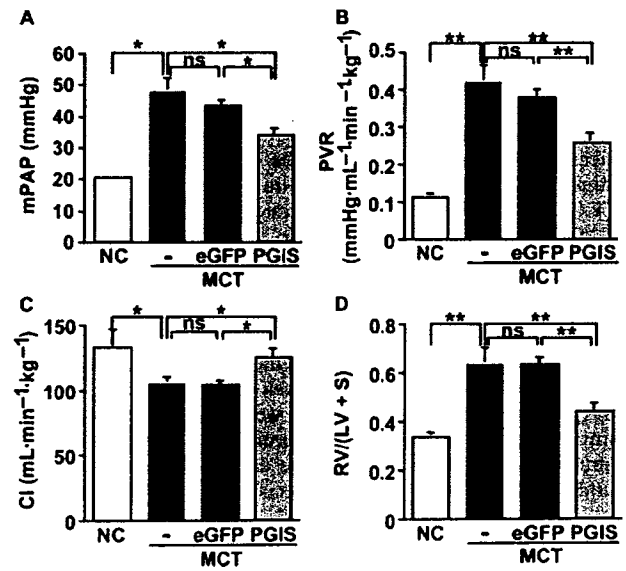

Figure 3. Effects of PGI_2 on hemodynamics and RVH. A quantitative analysis was performed using MCT-induced PAH rats 8 weeks after injecting the vector. A, mPAP (mm Hg); B, PVR (mm Hg · mL^{-1} · min^{-1} · kg^{-1}); C, CI (mL · min^{-1} · kg^{-1}). D, Weight ratio of the right ventricle to the left ventricle plus septum [RV/(LV+S)] presented as an index of RVH. Data are presented as means±SEM (n=4 to 10 animals per group). *$P<0.05$; **$P<0.01$. ns indicates not statistically significant; NC, untreated negative control.

Physiological and Laboratory Data of the MCT-Induced PAH Rats

Factor	NC	MCT	MCT+eGFP	MCT+PGIS	*P*
No. of rats	4	6	6	10	...
Heart rate, per minute	294.0±10.6	281.2±14.7	268.0±9.0	274.8±8.7	NS
ASAP, mm Hg	99.5±1.6	97.3±2.0	96.3±2.4	94.7±4.4	NS
Body weight, g	358.5±11.5	328.3±7.2	328.0±11.4	342.5±9.8	NS
Leukocyte, per mL	6725±372	7917±723	8800±849	8030±852	NS
Hematocrit, %	48.2±0.7	48.9±1.9	51.0±3.0	47.8±1.8	NS
Platelet, $\times 10^4/mm^3$	88.3±8.7	79.2±8.8	80.4±3.6	84.6±6.3	NS
ALT, IU/L	37.8±2.5	49.5±8.4	52.5±6.8	44.1±4.3	NS
Cr, mg/dL	0.52±0.04	0.59±0.05	0.48±0.03	0.53±0.04	NS

Data are presented as means±SEM (n=4 to 10 animals per group). ASAP indicates aortic systolic arterial pressure; ALT, serum alanine aminotransferase; Cr, serum creatinine; NS, not statistically significant.

medial thickness of the PA was greater in the MCT-administered rats than in the untreated controls (Figure 4A). Treatment with AAV-PGIS but not AAV-eGFP prevented the MCT-induced increase in the percentage of medial thickness significantly (Figure 4B, 25 to 50 μm; Figure 4C, 51 to 100 μm in external diameter).

Effects on the Survival of the MCT-PAH Rats and Their Organ Dysfunctions

The PGIS-transduced rats exhibited significantly improved survival rates as compared with the eGFP-transduced rats (Figure 5). The MCT administration produced a slight but not significant decrease in the body weight of the rats, and PGIS gene transfer prevented this decrease. Although the MCT group showed only a slight but not significant increase in the leukocyte count and serum alanine aminotransferase levels as compared with the NC group, the AAV-PGIS treatment caused no additional change in these parameters (Table).

Discussion

The present study demonstrates that sustained PGI_2 expression by a single intramuscular injection of AAV-PGIS prevents the development of MCT-PAH in rats. PGI_2 expression not only increased the cardiac output significantly but also prevented the progression of PVR, RVH, and medial hypertrophy of the PA that was induced by the MCT administration. The PGIS-transduced rats also exhibited significantly improved survival rates as compared with the controls. Furthermore, the PGIS expression observed in this study caused no additional adverse effects on hematologic data and serum indicators of hepatorenal function (alanine aminotransferase and creatinine levels) in the MCT-PAH rats.

The expression of PGI_2 and PGIS decreased in the remodeled PAs of the idiopathic PAH patients.[14,15] Impaired PGI_2 synthesis resulting from a decrease in PGIS expression may be implicated in the pathogenesis of PAH. In fact, continuous intravenous infusion of exogenous PGI_2 markedly lowers PVR and improves survival in PAH patients. However, this system requires lifelong infusion with a central venous catheter because of the short biological half-life of PGI_2. Furthermore, because this system is associated with life-threatening complications (eg, shock and sepsis) that may result in poor survival and quality of life of patients, stable

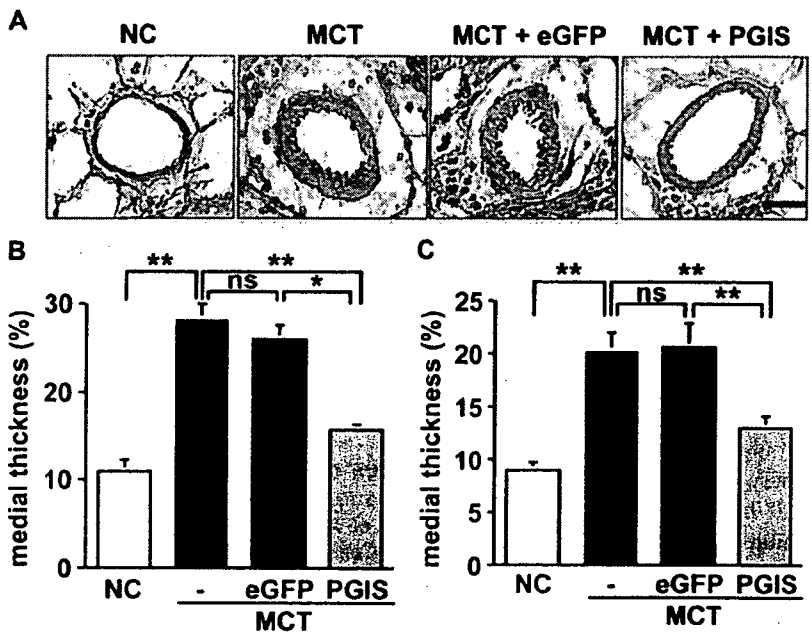

Figure 4. Effects of PGI_2 on medial hypertrophy of the peripheral PA. A, Representative cross-sections of the peripheral PA 4 weeks after the MCT administration (hematoxylin and eosin staining, original magnification, ×1000; scale bar=20 μm). B and C, Quantitative analysis of percentage of medial thickness (B, 25 to 50 μm; C, 51 to 100 μm in external diameter). Data are presented as means±SEM (n=4 to 10 animals per group). *$P<0.05$, **$P<0.01$. ns indicates not statistically significant; NC, untreated negative control.

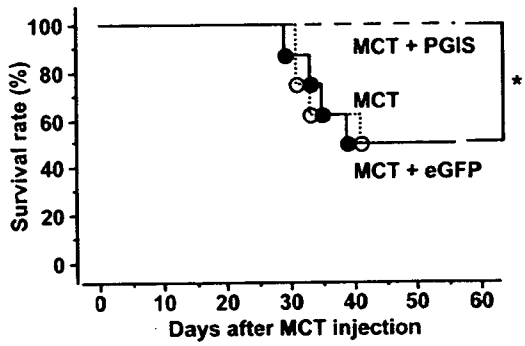

Figure 5. The survival rate of MCT-induced PAH rats. The rats were administered with MCT (40 mg/kg) 4 weeks after the injection of HN buffer (MCT group), AAV-eGFP (MCT+eGFP group), or AAV-PGIS (MCT+PGIS group). The rats were intramuscularly injected with the vectors at 1×10^{10} genome copies per body. The Kaplan-Meier method demonstrated a significant improvement in the survival rate of the rats in the MCT+PGIS group as compared with those in either the MCT or MCT+eGFP group at 8 weeks post-MCT administration. n=8 animals per group; *$P<0.05$ vs MCT or eGFP groups.

production of endogenous PGI_2 would be more desirable. Consistent with previous gene therapy studies, our strategy presented high levels of endogenous PGI_2 expression. In addition, this strategy caused no systemic hypotension and hyperdynamic heart failure, which are the major adverse effects arising from uncontrolled blood levels during intravenous delivery of exogenous PGI_2.[3,4,6]

In this study, we used an AAV serotype 1 vector because it is effective not only in efficient muscle transduction but also in long-term secretion of therapeutic proteins into the systemic circulation. The cDNA for human PGIS shares a high identity with its rat counterpart.[16] In fact, the administration of a plasmid or hemagglutinating virus of the Japan-liposome vector encoding human PGIS successfully ameliorated MCT-PAH. However, the use of these vectors requires repeated administration for achieving sustained gene expression.[3–5] In contrast, the AAV vector used in this study achieved PGIS expression with a single intramuscular injection, and this expression was sustained for 1 year.[7]

Furthermore, gene transfer was believed to be safer when performed via an intramuscular approach as opposed to the intratracheal or intrahepatic approaches.[6] Currently, researchers are using adenoviral gene transfer in most clinical trials because of its high efficiency for gene expression. However, the potential toxic effects of adenoviruses, such as strong immunogenicity, are well known. In contrast, the intramuscular administration of AAV vectors is a promising strategy for delivering therapeutic proteins safely and efficiently, and their use has been examined in clinical trials for hemophilia.[17]

Although PGI_2 is known to be a short-acting vasodilator, recent studies have shown its antiremodeling effects when used in high doses. The administration of PGI_2 analogues cicaprost and iloprost in high concentrations ($>10^{-7}$ mol/L) inhibits mitogen-induced proliferation of rat primary PA smooth muscle cells in a cAMP-dependent manner.[18] Interestingly, another PGI_2 analogue, treprostinil, also inhibits the proliferation of human and mouse primary lung fibroblasts through the activation of a peroxisome proliferator-activated receptor-β/δ when used in equivalent doses.[19] These observations suggest that high levels of PGI_2 may attenuate PA remodeling in vivo through antiproliferative effects. Consistent with previous studies, we demonstrated that high levels of endogenous PGI_2 successfully attenuated medial hypertrophy of the PA.[3,4,6] To discover new drug targets, the roles of peroxisome proliferator-activated receptors and high-level PGI_2 in PAH therapy should be determined, because peroxisome proliferator-activated receptors are associated with many inflammatory and proliferative disorders, including PAH.[2,20]

Finally, we will discuss the clinical implications and limitations of this study. Consistent with previous studies, maximum gene expression was noted 6 to 8 weeks after the intramuscular injection of AAV vectors. AAV-PGIS was injected 4 weeks before MCT administration for the transgene expression to reach plateau levels when MCT-PAH was fully developed (3 to 4 weeks after the injection). Our results are completely based on a preventive protocol, which may be rare in a clinical setting. However, PGI_2 is an established therapeutic molecule, and the advantage of early initiation of PGI_2 therapy for improving survival in patients with idiopathic PAH has been demonstrated in a large clinical trial.[21] These observations convinced us to propose the possible preemptive use of AAV-PGIS as a strategy to maintain basal levels of PGI_2 in patients with mild symptoms of PAH or in those identified as high-risk subjects who have not experienced PAH. As an alternative, the combined use of AAV-PGIS and an initial infusion of intravenous PGI_2 might be promising; the intravenous infusion should be tapered when sufficient levels of PGI_2 are attained. To evaluate the efficacy of AAV-PGIS in a therapeutic protocol (ie, vector injection after the development of PAH), use of a chronic hypoxic PAH model or newly developed self-complementary AAV vectors that can express transgenes earlier than the conventional vectors should be considered.[22]

Perspectives

The present study has demonstrated that the single intramuscular injection of AAV-PGIS achieved a sustained expression of PGI_2. This expression retarded the progression of MCT-PAH in rats without causing significant adverse effects. Thus, this strategy provides a new therapeutic alternative for PAH patients. However, the system in this study lacks the ability to regulate excessive transgene expression. Therefore, regulatory mechanisms to ensure adequate gene expression should be established to facilitate successful translation of this strategy in a clinical setting.

Acknowledgment

We thank Miyoko Mitsu for her encouragement and technical support.

Sources of Funding

This work was supported in part by grants from the Ministry of Health, Labor and Welfare of Japan; Grants-in-Aid for Scientific Research; grant for the 21st Century Centes of Excellence Program; "High-Tech Research Center" Project for Private Universities, matching fund subsidy, from the Ministry of Education, Culture,

Sports, Science and Technology of Japan; and the Research Award to Jichi Medical School Graduate Student.

Disclosures

None.

References

1. Humbert M, Sitbon O, Simonneau G. Treatment of pulmonary arterial hypertension. *N Engl J Med.* 2004;351:1425–1436.
2. Ito T, Ozawa K, Shimada K. Current drug targets and future therapy of pulmonary arterial hypertension. *Curr Med Chem.* 2007;14:719–733.
3. Nagaya N, Yokoyama C, Kyotani S, Shimonishi M, Morishita R, Uematsu M, Nishikimi T, Nakanishi N, Ogihara T, Yamagishi M, Miyatake K, Kaneda Y, Tanabe T. Gene transfer of human prostacyclin synthase ameliorates monocrotaline-induced pulmonary hypertension in rats. *Circulation.* 2000;102:2005–2010.
4. Suhara H, Sawa Y, Fukushima N, Kagisaki K, Yokoyama C, Tanabe T, Ohtake S, Matsuda H. Gene transfer of human prostacyclin synthase into the liver is effective for the treatment of pulmonary hypertension in rats. *J Thorac Cardiovasc Surg.* 2002;123:855–861.
5. Ono M, Sawa Y, Mizuno S, Fukushima N, Ichikawa H, Bessho K, Nakamura T, Matsuda H. Hepatocyte growth factor suppresses vascular medial hyperplasia and matrix accumulation in advanced pulmonary hypertension of rats. *Circulation.* 2004;110:2896–2902.
6. Tahara N, Kai H, Niiyama H, Mori T, Sugi Y, Takayama N, Yasukawa H, Numaguchi Y, Matsui H, Okumura K, Imaizumi T. Repeated gene transfer of naked prostacyclin synthase plasmid into skeletal muscles attenuates monocrotaline-induced pulmonary hypertension and prolongs survival in rats. *Hum Gene Ther.* 2004;15:1270–1278.
7. Yoshioka T, Okada T, Maeda Y, Ikeda U, Shimpo M, Nomoto T, Takeuchi K, Nonaka-Sarukawa M, Ito T, Takahashi M, Matsushita T, Mizukami H, Hanazono Y, Kume A, Ookawara S, Kawano M, Ishibashi S, Shimada K, Ozawa K. Adeno-associated virus vector-mediated interleukin-10 gene transfer inhibits atherosclerosis in apolipoprotein E-deficient mice. *Gene Ther.* 2004;11:1772–1779.
8. Chen S, Kapturczak MH, Wasserfall C, Glushakova OY, Campbell-Thompson M, Deshane JS, Joseph R, Cruz PE, Hauswirth WW, Madsen KM, Croker BP, Berns KI, Atkinson MA, Flotte TR, Tisher CC, Agarwal A. Interleukin 10 attenuates neointimal proliferation and inflammation in aortic allografts by a heme oxygenase-dependent pathway. *Proc Natl Acad Sci U S A.* 2005;102:7251–7256.
9. Mu W, Ouyang X, Agarwal A, Zhang L, Long DA, Cruz PE, Roncal CA, Glushakova OY, Chiodo VA, Atkinson MA, Hauswirth WW, Flotte TR, Rodriguez-Iturbe B, Johnson RJ, Ii.-10 suppresses chemokines, inflammation, and fibrosis in a model of chronic renal disease. *J Am Soc Nephrol.* 2005;16:3651–3660.
10. Matsushita T, Elliger S, Elliger C, Podsakoff G, Villarreal L, Kurtzman GJ, Iwaki Y, Colosi P. Adeno-associated virus vectors can be efficiently produced without helper virus. *Gene Ther.* 1998;5:938–945.
11. Okada T, Nomoto T, Yoshioka T, Nonaka-Sarukawa M, Ito T, Ogura T, Iwata-Okada M, Uchibori R, Shimazaki K, Mizukami H, Kume A, Ozawa K. Large-scale production of recombinant viruses by use of a large culture vessel with active gassing. *Hum Gene Ther.* 2005;16:1212–1218.
12. Okada T, Nomoto T, Shimazaki K, Lijun W, Lu Y, Matsushita T, Mizukami H, Urabe M, Hanazono Y, Kume A, Muramatsu S, Nakano I, Ozawa K. Adeno-associated virus vectors for gene transfer to the brain. *Methods.* 2002;28:237–247.
13. Kay JM, Keane PM, Suyama KL, Gauthier D. Angiotensin converting enzyme activity and evolution of pulmonary vascular disease in rats with monocrotaline pulmonary hypertension. *Thorax.* 1982;37:88–96.
14. Christman BW, McPherson CD, Newman JH, King GA, Bernard GR, Groves BM, Loyd JE. An imbalance between the excretion of thromboxane and prostacyclin metabolites in pulmonary hypertension. *N Engl J Med.* 1992;327:70–75.
15. Tuder RM, Cool CD, Geraci MW, Wang J, Abman SH, Wright L, Badesch D, Voelkel NF. Prostacyclin synthase expression is decreased in lungs from patients with severe pulmonary hypertension. *Am J Respir Crit Care Med.* 1999;159:1925–1932.
16. Miyata A, Hara S, Yokoyama C, Inoue H, Ullrich V, Tanabe T. Molecular cloning and expression of human prostacyclin synthase. *Biochem Biophys Res Commun.* 1994;200:1728–1734.
17. High K. AAV-mediated gene transfer for hemophilia. *Genet Med.* 2002; 4:56S–61S.
18. Phillips PG, Long L, Wilkins MR, Morrell NW. cAMP phosphodiesterase inhibitors potentiate effects of prostacyclin analogs in hypoxic pulmonary vascular remodeling. *Am J Physiol Lung Cell Mol Physiol.* 2005;288: L103–L115.
19. Ali FY, Egan K, FitzGerald GA, Desvergne B, Wahli W, Bishop-Bailey D, Warner TD, Mitchell JA. Role of prostacyclin versus peroxisome proliferator-activated receptor beta receptors in prostacyclin sensing by lung fibroblasts. *Am J Respir Cell Mol Biol.* 2006;34:242–246.
20. Ameshima S, Golpon H, Cool CD, Chan D, Vandivier RW, Gardai SJ, Wick M, Nemenoff RA, Geraci MW, Voelkel NF. Peroxisome proliferator-activated receptor gamma (PPARgamma) expression is decreased in pulmonary hypertension and affects endothelial cell growth. *Circ Res.* 2003;92:1162–1169.
21. Sitbon O, Humbert M, Nunes H, Parent F, Garcia G, Herve P, Rainisio M, Simonneau G. Long-term intravenous epoprostenol infusion in primary pulmonary hypertension: prognostic factors and survival. *J Am Coll Cardiol.* 2002;40:780–788.
22. Nathwani AC, Gray JT, McIntosh J, Ng CY, Zhou J, Spence Y, Cochrane M, Gray E, Tuddenham EG, Davidoff AM. Safe and efficient transduction of the liver after peripheral vein infusion of self-complementary AAV vector results in stable therapeutic expression of human FIX in nonhuman primates. *Blood.* 2007;109:1414–1421.

ELSEVIER

International Journal of Cardiology 119 (2007) 344–348

International Journal of Cardiology

www.elsevier.com/locate/ijcard

Circulating endothelial progenitor cells in congestive heart failure ☆

Mutsuko Nonaka-Sarukawa [a], Keiji Yamamoto [a,*], Hirotaka Aoki [a], Yoshioki Nishimura [a], Hidenori Tomizawa [a], Masaru Ichida [a], Takayuki Eizawa [a], Kazuo Muroi [b], Uichi Ikeda [c], Kazuyuki Shimada [a]

[a] *Division of Cardiovascular Medicine, Jichi Medical University, Shimotsuke, Tochigi 329-0498, Japan*
[b] *Division of Cell Transplantation and Transfusion, Jichi Medical University, Shimotsuke, Tochigi 329-0498, Japan*
[c] *Department of Organ Regeneration, Shinshu University Graduate School of Medicine, Matsumoto, Nagano 390-8621, Japan*

Received 9 June 2006; accepted 29 July 2006
Available online 27 October 2006

Abstract

Background: Endothelial progenitor cells (EPCs) circulate in the adult peripheral blood and contribute to neovascularization. EPCs are considered to be included in CD34 positive mononuclear cells ($CD34^+$ MNCs). Kinetics of circulating EPCs in congestive heart failure (CHF) has not been fully investigated.

Methods: We determined the numbers of white blood cells (WBCs), plasma brain natriuretic peptide (BNP), serum erythropoietin, vascular endothelial growth factor (VEGF) and thrombomodulin levels in 16 mild CHF patients (NYHA I, II), 10 severe CHF patients with acute exacerbation (NYHA III, IV), and 22 control subjects. The number of $CD34^+$ MNCs in peripheral blood was quantified by flow cytometry.

Results: The ratio of $CD34^+$ MNCs:10^3 WBCs in mild CHF patients was higher than that in control subjects ($P<0.05$). Interestingly, the ratio of $CD34^+$ MNCs:10^3 WBCs in severe CHF patients at admission was significantly lower than that in control subjects ($P<0.005$) or in mild CHF patients ($P<0.05$). Levels of BNP and erythropoietin in severe CHF patients were significantly higher than those in mild CHF patients. However, VEGF and thrombomodulin levels were not different between mild and severe CHF patients. In addition, the ratio of $CD34^+$ MNCs:10^3 WBCs in severe CHF patients increased in proportion to the amelioration of CHF during hospitalization, and this increase correlated with the decrease in BNP level.

Conclusions: The ratio of $CD34^+$ MNCs:10^3 WBCs was decreased in severe CHF. These findings suggest that impaired EPC recruitment might be involved in the pathophysiology of severe CHF.

Keywords: Heart failure; Endothelial progenitor cells; Brain natriuretic peptide

1. Introduction

The bone marrow-derived endothelial progenitor cells (EPCs) are considered to originate from hematopoietic stem cells, which are positive for CD34 [1,2]. Circulating EPCs home to sites of neovascularization and differentiate into endothelial cells in site [3,4] in a manner consistent with a process termed vasculogenesis [5]. EPCs and $CD34^+$ cells increase in patients with endothelial damage [6], vascular trauma [7], and acute myocardial infarction [8], which reflects increased endothelial cell turnover. Local or systemic administration of cultured or fresh EPCs enhances ischemic neovascularization and improves function of ischemic tissues in animals with hindlimb or myocardial ischemia [9,10]. Recently, the therapeutic benefits of EPC therapy were demonstrated in patients with severe ischemia in the lower limb and with acute myocardial infarction [11,12].

Despite recent therapeutic advances, congestive heart failure (CHF) leading to high mortality is a major health problem [13]. During progression to overt heart failure,

☆ This study was supported in part by a grant from the Ministry of Education, Culture, Sports, Science, and Technology of Japan (15590769), Tokyo, Japan.
* Corresponding author. Tel.: +81 285 58 7344; fax: +81 285 44 5317.
E-mail address: kyamamoto@jichi.ac.jp (K. Yamamoto).

0167-5273/$ - see front matter © 2006 Elsevier Ireland Ltd. All rights reserved.
doi:10.1016/j.ijcard.2006.07.191

Table 1
Characteristics of patients with CHF

	Control	NYHA I or II	NYHA III or IV
Male/female (*n*)	16/6	8/8	6/4
Age (yrs)	52±11	57±12	68±10
NYHA functional class (n)			
I/II		7/9	
III/IV			3/7
LVEF (%)		48±18	34±15
Underlying heart disease (*n*)			
Idiopathic dilated cardiomyopathy		4	3
Valvular heart disease		5	2
Healed myocardial infarction		0	2
Hypertensive heart disease		1	1
Arrhythmia		3	2
Others		3	0
Smoking (*n*)		3	5
Diabetes mellitus (*n*)		2	4
Hypercholesterolemia (*n*)		3	2
Drugs (*n*)			
Nitrate		2	2
Calcium antagonist		3	2
Beta-blocker		6	0
ACE inhibitor		11	2
Digoxin		6	2
Diuretic		12	6

Values are mean±SEM or number of patients. ACE, angiotensin-converting enzyme; CHF, congestive heart failure; LVEF, left ventricular ejection fraction; NYHA, New York Heart Association.

reduced cardiac output and concomitant neuroendocrine activation affect the functions of several organs. Patients with heart failure show endothelial dysfunction. In heart failure, nitric oxide production is diminished, whereas rate of endothelial apoptosis is increased [14]. Recently, a mobilization of EPCs into circulation from bone marrow has been reported in patients with acute myocardial infarction and acute coronary syndrome [8]. However, little is known about the kinetics of EPC mobilization in patients with CHF, especially the course of EPC mobilization in severe CHF.

In the present study, we measured the number of $CD34^+$ mononuclear cells (MNCs), plasma brain natriuretic peptide (BNP), serum erythropoietin, vascular endothelial growth factor (VEGF) and thrombomodulin, a marker of endothelial damage, levels to elucidate the kinetics of EPC mobilization in patients with CHF.

2. Methods

2.1. Study patients

We studied 16 mild CHF outpatients with New York Heart Association (NYHA) functional class I or II (8 men and 8 women, mean age 57±12 years) and 10 severe CHF patients with NYHA functional class III or IV (6 men and 4 women, mean age 68±10 years) admitted to our hospital for acute exacerbation of CHF (Table 1). The diagnosis of heart failure was confirmed in all patients by clinical findings and noninvasive assessment of cardiac function. Left ventricular ejection fraction was determined by echocardiographic evaluation [15]. Patients with coronary artery disease were excluded by angiographic findings and/or clinical history. Patients with renal failure, infection, chronic inflammatory disease and malignancy were excluded from this study. The control group consisted of 22 healthy volunteers (16 men and 6 women, mean age 52±11 years) without cardiovascular disease. This study was approved by our institutional human investigations committee, and written informed consent was obtained from all patients and volunteers before participation.

2.2. Blood collection

In severe CHF patients with acute exacerbation of CHF, sampling was performed at admission (on day 1), and on 14 days after admission. Blood sampling was performed after a 12-hour fast. All the subjects were supine, and a 21-gauge needle was inserted into a large antecubital vein. A 5-ml sample of whole blood for plasma separation was drawn into a plastic tube containing 7.5 mg Na_2-ethylenediaminetetraacetic acid. Plasma and serum were separated by prompt centrifugation of the blood samples at 3000 ×*g* at 4 °C for 10 min. The samples were immediately frozen, and stored at −80 °C.

2.3. Flow cytometry analysis

The number of $CD34^+$ MNCs in the peripheral blood was quantified using flow cytometry (Cytron; Ortho Diagnostic Systems) [16]. In brief, white blood cells (WBCs) were dually stained with fluorescent isothiocyanate (FITC)-conjugated CD45 (Becton Dickinson Immunocytometry Systems) and phycoerythrin (PE)-conjugated CD34 (Becton). Progenitors were separated by CD45 expression and right-angle light scatter properties. Cells expressing CD34 were measured with gating on the progenitor population. For negative

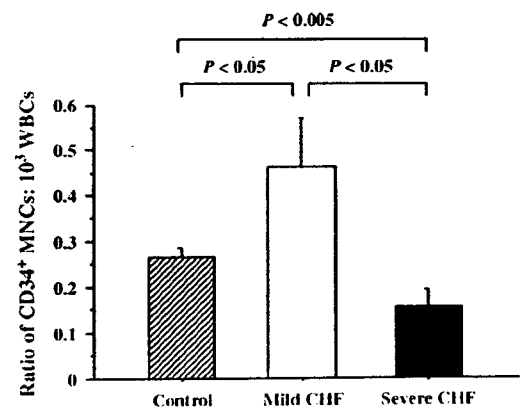

Fig. 1. The number of circulating $CD34^+$ MNCs in CHF patients. The $CD34^+$ MNC counts in control subjects (n=22), mild CHF patients with New York Heart Association (NYHA) functional class I or II (n=16) and severe CHF patients with NYHA functional class III or IV (n=10) were determined by two-color flow cytometry. Results are shown as means± SEM.

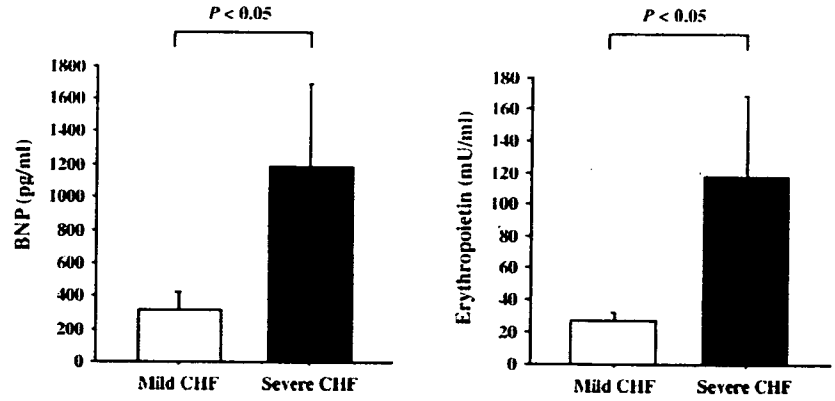

Fig. 2. Plasma BNP and serum erythropoietin levels in CHF patients. Results are shown as means±SEM.

controls, cells were stained with FITC-conjugated CD45 and PE-conjugated mouse IgG1 (Becton).

2.4. Measurements of BNP, erythropoietin, VEGF and thrombomodulin

The levels of plasma BNP and serum erythropoietin were determined by radioimmunoassay (SRL Inc., Tokyo, Japan), respectively. The sensitivity of the assays for BNP and erythropoietin was 2.0 pg/ml and 5.0 mU/ml, respectively. The levels of serum VEGF were measured using a specific enzyme-linked immunosorbent assay kit (R&D Systems) as reported previously [17]. The sensitivity of the assays for serum VEGF was 9 pg/ml. The serum levels of thrombomodulin were determined using the one-step sandwich enzyme immunoassay kit (Fuji Chemical Industries Ltd., Takaoka, Japan). The sensitivity of the assays for thrombomodulin was 1.1 FU/ml.

2.5. Statistical analysis

Data are expressed as mean±SEM. The data were analyzed by nonparametric methods to avoid assumptions about the distribution of the measured variables. ANOVA was performed with the Kruskal–Wallis method. Subsequent pairwise comparisons were made with the Mann–Whitney *U* test. The differences between baseline and posttreatment values were analyzed with the Wilcoxon signed rank test. Moreover, the association of $CD34^+$ MNCs:10^3 WBCs with other biochemical parameters was assessed by the Spearman rank correlation test. A *P*-value of <0.05 was considered significant.

3. Results

3.1. Circulating $CD34^+$ MNCs

As illustrated in Fig. 1, the ratio of $CD34^+$ MNCs:10^3 WBCs in mild CHF patients (0.46±0.11) was significantly higher than that in control subjects (0.27±0.02, $P<0.05$). Interestingly, the ratio of $CD34^+$ MNCs:10^3 WBCs in severe CHF patients at admission (0.16±0.04) was significantly lower than that in control subjects ($P<0.005$) or in mild CHF patients ($P<0.05$).

3.2. Levels of BNP, erythropoietin, VEGF and thrombomodulin in CHF

As previously reported, level of BNP, a marker of morbidity and prognostic indicators in CHF [18,19], in severe CHF patients (1183±505 pg/ml) was significantly higher

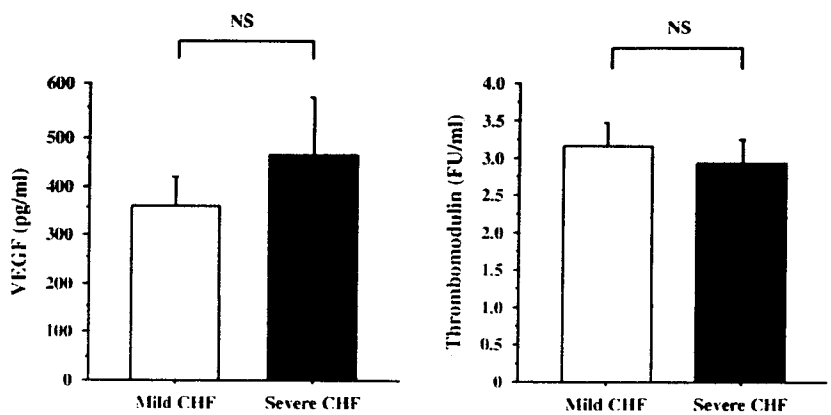

Fig. 3. Serum VEGF and thrombomodulin levels in CHF patients. Results are shown as means±SEM.

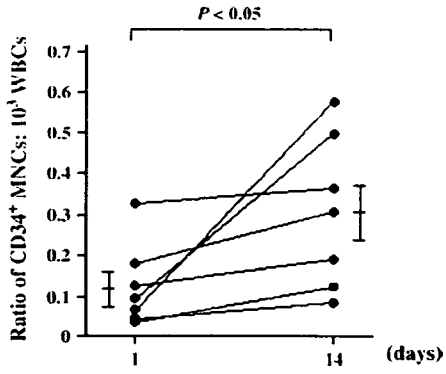

Fig. 4. The number of circulating $CD34^+$ MNCs during hospitalization in severe CHF patients. The $CD34^+$ MNC counts were determined by two-color flow cytometry. The data on day 1 represent the number of circulating $CD34^+$ MNCs in the severe CHF patients ($n=7$) at admission. Results are shown as means±SEM.

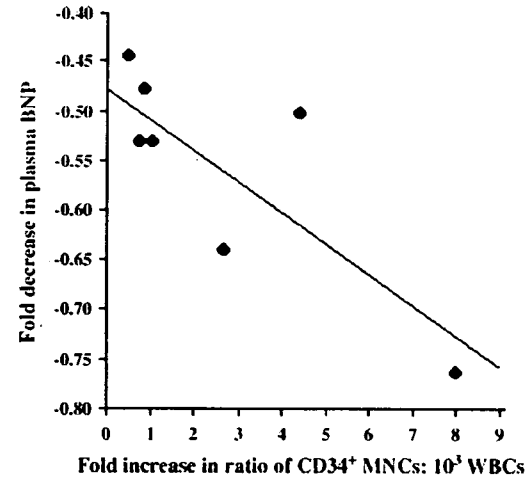

Fig. 6. Relation between increase in circulating $CD34^+$ MNCs and decrease in level of BNP. There was a high relation between increase in circulating $CD34^+$ MNCs and decrease in level of BNP during hospitalization in severe CHF ($y=-0.031x-0.48$, $r=-0.79$, $P=0.06$, $n=7$).

than that in mild CHF patients (306±117, $P<0.05$, Fig. 2). Next, we measured levels of erythropoietin and VEGF, physiologic stimuli for EPC mobilization [20,21], in CHF. Level of erythropoietin (117±52 mU/ml) in severe CHF patients was significantly higher than that (27±5, $P<0.05$) in mild CHF patients (Fig. 2). In contrast, serum VEGF level was not different between mild and severe CHF patients (355± 58 pg/ml vs. 456±116, $P=0.40$, Fig. 3). Level of thrombomodulin, a marker of endothelial damage, was not different between mild and severe CHF patients (3.2±0.3 FU/ml vs. 3.0± 0.3, $P=0.66$, Fig. 3).

3.3. Circulating $CD34^+$ MNCs and levels of BNP and erythropoietin during hospitalization in severe CHF

As shown in Fig. 4, the ratio of $CD34^+$ MNCs:10^3 WBCs in severe CHF patients (0.12±0.04) significantly increased in proportion to the amelioration of CHF during hospitalization (0.30±0.07 on 14 days after admission, $P<0.05$). In contrast, levels of BNP and erythropoietin (BNP, 1494±700 pg/ml; erythropoietin, 79±22 mU/ml) decreased in proportion to the amelioration of CHF during hospitalization (BNP, 529±162; erythropoietin, 24±6 on 14 days after admission, Fig. 5). This increase in ratio of $CD34^+$ MNCs:10^3 WBCs during hospitalization in severe CHF patients correlated with the decrease in BNP level ($y=-0.031x-0.48$, $r=-0.79$, $P=0.06$, Fig. 6).

4. Discussion

In the present study, we investigated the kinetics of circulating EPCs in CHF. We found that the number of EPCs, as measured by the number of cells expressing CD34 was significantly reduced in severe CHF patients with acute exacerbation and increased in proportion to the amelioration of CHF during hospitalization. These findings suggest that impaired EPC recruitment might be involved in the pathophysiology of severe CHF.

The mechanisms by which the condition of CHF modulates $CD34^+$ cell numbers remain to be determined. In this study, the number of $CD34^+$ MNCs significantly increased in mild CHF patients and was significantly reduced in severe

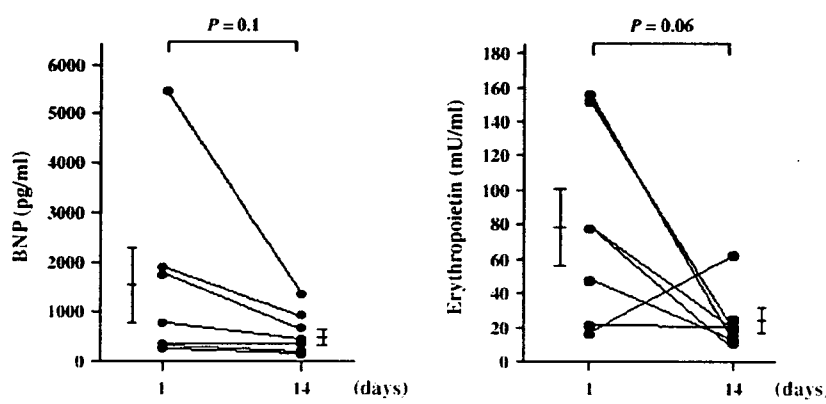

Fig. 5. Plasma BNP and serum erythropoietin levels during hospitalization in severe CHF patients. The data on day 1 represent the BNP and erythropoietin levels in the severe CHF patients at admission. Results are shown as means±SEM.

CHF patients with acute exacerbation. Injury to the heart causes hematopoietic progenitor cells to migrate to the site of damage and to undergo progenitor cell differentiation [22,23]. This mechanism may contribute to the increase in $CD34^-$ MNCs observed in mild CHF patients. Iversen et al. [24] found decreased hematopoiesis in bone marrow of mice with CHF. In severe CHF, suppressed bone marrow function may lead to decrease in $CD34^+$ MNCs. An exhaustion of progenitor cells in the advanced phases of the disease could contribute to the biphasic bone marrow pattern of response to heart failure.

Increasing evidence suggests several growth factors and cytokines formerly thought to be specific for the hematopoietic system. Serum levels of erythropoietin and VEGF are associated with the number of stem and progenitor cells in the bone marrow as well as the number and function of circulating EPCs [21]. In this study, we investigated levels of erythropoietin and VEGF, two potent physiologic stimuli for EPC mobilization. Level of erythropoietin in severe CHF patients was significantly higher than that in mild CHF patients, but not serum VEGF level. These findings suggest that bone marrow suppression in severe CHF secondarily may induce the increase in erythropoietin level. In addition, the levels of serum thrombomodulin were not different between mild and severe CHF patients. These observations suggest that endothelial damage in CHF is unlikely related to the modulation of circulating $CD34^-$ MNCs.

In conclusion, the present study demonstrated that the number of $CD34^+$ MNCs was decreased in severe CHF and increased in proportion to the amelioration of CHF during hospitalization. These findings suggest that impaired EPC recruitment might be involved in the pathophysiology of severe CHF and that a method of increasing $CD34^+$ MNCs may be a novel therapeutic strategy in severe CHF.

Acknowledgement

This study was supported in part by a grant from the Ministry of Education, Culture, Sports, Science, and Technology of Japan (15590769), Tokyo, Japan.

References

[1] Asahara T, Murohara T, Sullivan A, et al. Isolation of putative progenitor endothelial cells for angiogenesis. Science 1997;275:964–7.
[2] Bhattacharya V, McSweeney PA, Shi Q, et al. Enhanced endothelialization and microvessel formation in polyester grafts seeded with CD34(+) bone marrow cells. Blood 2000;95:581–5.
[3] Shi Q, Rafii S, Wu MH, et al. Evidence for circulating bone marrow-derived endothelial cells. Blood 1998;92:362–7.
[4] Takahashi T, Kalka C, Masuda H, et al. Ischemia- and cytokine-induced mobilization of bone marrow-derived endothelial progenitor cells for neovascularization. Nat Med 1999;5:434–8.
[5] Carmeliet P. Mechanisms of angiogenesis and arteriogenesis. Nat Med 2000;6:389–95.
[6] Hill JM, Zalos G, Halcox JP, et al. Circulating endothelial progenitor cells, vascular function and cardiovascular risk. N Engl J Med 2003;348:593–600.
[7] Gill M, Dias S, Hattori K, et al. Vascular trauma induces rapid but transient mobilization of $VEGFR2^+AC133^+$ endothelial precursor cells. Circ Res 2001;88:167–74.
[8] Shintani S, Murohara T, Ikeda H, et al. Mobilization of endothelial progenitor cells in patients with acute myocardial infarction. Circulation 2001;103:2776–9.
[9] Asahara T, Masuda H, Takahashi T, et al. Bone marrow origin of endothelial progenitor cells responsible for postnatal vasculogenesis in physiological and pathological neovascularization. Circ Res 1999;85:221–8.
[10] Murohara T, Ikeda H, Duan J, et al. Transplanted cord blood-derived endothelial precursor cells augment postnatal neovascularization. J Clin Invest 2000;105:1527–36.
[11] Tateishi-Yuyama E, Matsubara H, Murohara T, et al. Therapeutic angiogenesis for patients with limb ischaemia by autologous transplantation of bone-marrow cells: a pilot study and a randomised controlled trial. Lancet 2002;360:427–35.
[12] Inaba S, Egashira K, Komori K. Peripheral-blood or bone-marrow mononuclear cells for therapeutic angiogenesis? Lancet 2002;360:2083.
[13] Ho KK, Anderson KM, Kannel WB, et al. Survival after the onset of congestive heart failure in Framingham Heart Study subjects. Circulation 1993;88:107–15.
[14] Agnoletti L, Curello S, Bachetti T, et al. Serum from patients with severe heart failure downregulates eNOS and is proapoptotic: role of tumor necrosis factor-alpha. Circulation 1999;100:1983–91.
[15] Schiller NB, Acquatella H, Ports TA, et al. Left ventricular volume from paired biplane two-dimensional echocardiography. Circulation 1979;60:547–55.
[16] Sutherland DR, Anderson L, Keeney M, et al. The ISHAGE guidelines for $CD34^+$ cell determination by flow cytometry. J Hematother 1996;5:213–26.
[17] Hojo Y, Ikeda U, Zhu Y, et al. Expression of vascular endothelial growth factor in patients with acute myocardial infarction. J Am Coll Cardiol 2000;35:968–73.
[18] Omland T, Aakvaag A, Bonarjee VV, et al. Plasma brain natriuretic peptide as an indicator of left ventricular systolic function and long-term survival after acute myocardial infarction. Comparison with plasma atrial natriuretic peptide and N-terminal proatrial natriuretic peptide. Circulation 1996;93:1963–9.
[19] Nonaka-Sarukawa M, Yamamoto K, Aoki H, et al. Increased urinary 15-F2t-isoprostane concentrations in patients with non-ischaemic congestive heart failure: a marker of oxidative stress. Heart 2003;89:871–4.
[20] Heeschen C, Aicher A, Lehmann R, et al. Erythropoietin is a potent physiologic stimulus for endothelial progenitor cell mobilization. Blood 2003;102:1340–6.
[21] Yoon YS, Johnson IA, Park JS, et al. Therapeutic myocardial angiogenesis with vascular endothelial growth factors. Mol Cell Biochem 2004;264:63–74.
[22] Kocher AA, Schuster MD, Szabolcs MJ, et al. Neovascularization of ischemic myocardium by human bone-marrow-derived angioblasts prevents cardiomyocyte apoptosis, reduces remodeling and improves cardiac function. Nat Med 2001;7:430–6.
[23] Quaini F, Urbanek K, Beltrami AP, et al. Chimerism of the transplanted heart. N Engl J Med 2002;346:5–15.
[24] Iversen PO, Woldbaek PR, Tonnessen T, et al. Decreased hematopoiesis in bone marrow of mice with congestive heart failure. Am J Physiol Regul Integr Comp Physiol 2002;282:R166–72.

Arteriosclerosis, Thrombosis, and Vascular Biology

JOURNAL OF THE AMERICAN HEART ASSOCIATION

M-CSF Accelerates Neointimal Formation in the Early Phase After Vascular Injury in Mice: The Critical Role of the SDF-1–CXCR4 System

Yuji Shiba, Masafumi Takahashi, Toru Yoshioka, Noriyuki Yajima, Hajime Morimoto, Atsushi Izawa, Hirohiko Ise, Kiyohiko Hatake, Kazuo Motoyoshi and Uichi Ikeda

Arterioscler. Thromb. Vasc. Biol. 2007;27;283-289; originally published online Oct 19, 2006;
DOI: 10.1161/01.ATV.0000250606.70669.14
Arteriosclerosis, Thrombosis, and Vascular Biology is published by the American Heart Association. 7272 Greenville Avenue, Dallas, TX 72514
 Print ISSN: 1079-5642. Online ISSN: 1524-4636

M-CSF Accelerates Neointimal Formation in the Early Phase After Vascular Injury in Mice

The Critical Role of the SDF-1–CXCR4 System

Yuji Shiba, Masafumi Takahashi, Toru Yoshioka, Noriyuki Yajima, Hajime Morimoto, Atsushi Izawa, Hirohiko Ise, Kiyohiko Hatake, Kazuo Motoyoshi, Uichi Ikeda

Objective—Since the macrophage colony-stimulating factor (M-CSF) has been shown to stimulate differentiation and proliferation of monocyte/macrophage lineage and to be involved in the process of neointimal formation after vascular injury, we tested the effects of M-CSF on the recruitment of bone marrow–derived progenitor cells in neointimal formation after vascular injury in mice.

Methods and Results—Wire-mediated vascular injury was produced in the femoral artery of C57BL/6 mice. Recombinant human M-CSF [500 μg/(kg·day)] or saline (control) was administered for 10 consecutive days, starting 4 days before the injury. Treatment with M-CSF accelerated neointimal formation in the early phase after injury, and this neointimal lesion mainly consisted of bone marrow–derived cells. M-CSF treatment had no effect on the mobilization of endothelial progenitor cells (EPCs: $CD34^+/Flk\text{-}1^+$) and reendothelialization after injury. The stromal cell-derived factor-1 (SDF-1) was markedly expressed in the neointima and media after injury, whereas $CXCR4^+$ cells were observed in the neointima. Further, a novel CXCR4 antagonist, AMD3100, significantly attenuated the M-CSF–induced neointimal formation.

Conclusions—These findings suggest that M-CSF accelerated neointimal formation after vascular injury via the SDF-1–CXCR4 system, and the inhibition of this system has therapeutic potential for the treatment of cardiovascular diseases. (***Arterioscler Thromb Vasc Biol.* 2007;27:283-289.**)

Key Words: angioplasty ■ cytokines ■ inflammation ■ restenosis ■ vascular biology

The vascular endothelium forms a biological interface between circulating blood components and various tissues in the body. This monolayer of endothelial cells locally monitors systemically generated stimuli, and alters the functional state of the vessels. This adaptive mechanism contributes to normal homeostasis; however, nonadaptive changes in the endothelial structure and function, provoked by pathophysiological stimuli, may induce "endothelial dysfunction," which plays an important role in the initiation and progression of cardiovascular diseases. In particular, the loss of endothelial cells because of vascular injury leads to the migration and proliferation of vascular smooth muscle cells (SMCs), resulting in neointimal formation. Further, the vascular injury initiates an inflammatory healing response that involves the expression of growth factors and cytokines and promotes neointimal formation. The resultant neointimal formation is the pathological basis of atherosclerosis and restenosis following percutaneous coronary intervention (PCI) such as angioplasty and stenting.

See page 263

The recruitment, activation, and proliferation of monocytes/macrophages in the vessel wall make important contribution to the process of atherosclerosis and restenosis. The presence of activated monocytes/macrophages at the site of the vascular injury leads to the release of vasoactive molecules, cytokines, and growth factors, which can induce the migration and proliferation of SMCs. However, recent evidence indicates that a part of the population of endothelial progenitor cells (EPCs) are derived from the monocyte/macrophage lineage cells, and these participate in the neovascularization of ischemic tissues.[1–3] In addition, monocyte/macrophage lineage-derived EPCs secrete large amounts of angiogenic factors, such as vascular endothelial growth factor (VEGF) and hepatocyte growth factor (HGF)[3]; this suggests that monocytes/macrophages can promote neovascularization. Further, the bone marrow–derived EPCs may contribute to the process of reendothelialization, termed "vascular repair," and prevent neointimal formation after vascular injury.[4]

Original received July 24, 2006; final version accepted September 28, 2006.

From the Division of Cardiovascular Sciences, Department of Organ Regeneration (Y.S., M.T., T.Y., N.Y., H.M., A.I., H.I., U.I.), Shinshu University Graduate School of Medicine, Matsumoto; the Cancer Chemotherapy Center (K.H.), Japanese Foundation for Cancer Research, Tokyo; and the Third Department of Internal Medicine (K.M.), National Defense Medical College, Saitama, Japan.

Correspondence to Masafumi Takahashi, MD, PhD, Division of Cardiovascular Sciences, Department of Organ Regeneration, Shinshu University Graduate School of Medicine, 3-1-1 Asahi, Matsumoto, Nagano 390-8621, Japan. E-mail masafumi@sch.md.shinshu-u.ac.jp

Arterioscler Thromb Vasc Biol. is available at http://www.atvbaha.org

DOI: 10.1161/01.ATV.0000250606.70669.14

However, it remains unclear whether the monocyte/macrophage lineage cells play a substantial role in neointimal formation after vascular injury.

The macrophage colony-stimulating factor (M-CSF) is a multifunctional proinflammatory cytokine that regulates the differentiation, proliferation, and survival of monocytic progenitor cells,[5] and plays a role in the differentiation of monocytes to macrophages in the arterial wall. Recent investigations suggest that M-CSF plays an important role in human atherosclerotic lesions[6,7] and in experimental animal models of atherosclerosis[8,9]; M-CSF activates monocytes/macrophages and promotes the proliferation of these cells and SMCs. Further, an increased expression of M-CSF after vascular injury has been demonstrated.[10] We previously reported that in patients with coronary artery diseases, M-CSF levels in the coronary sinus blood increased after PCI, and this increase was related to the development of restenosis.[11]

In the present study, we postulate that M-CSF might play a role in the mobilization of bone marrow–derived progenitor cells, reendothelialization, and neointimal formation after vascular injury. We demonstrated that exogenous M-CSF treatment accelerated neointimal formation in the early phase after vascular injury, and this formation was mediated through a system comprising a key stem cell homing factor, stromal cell–derived factor (SDF-1: CXCL12), and the SDF-1 receptor CXCR4. The findings obtained from this study may provide new insights into the role of M-CSF and the SDF-1–CXCR4 system in the pathogenesis of neointimal formation after vascular injury.

Materials and Methods

All materials and methods are detailed in the online supplement available at http://atvb.ahajournals.org.

Results

Effect of M-CSF on Neointimal Formation After Vascular Injury

We first assessed whether M-CSF was upregulated in the site of vascular injury, and found the expression of M-CSF at the injured artery (Figure 1A). Previously, we demonstrated that neointimal formation is initiated at 7 days and completed at 21 days after wire-mediated vascular injury in mice.[12] Hence, we evaluated the effect of M-CSF treatment on neointimal formation 7, 14, and 21 days after vascular injury. As expected, histological analysis showed that neointimal formation was initiated on the 7th day; it increased until the 14th day, and was completed by the 21st day after the injury in control mice (Figure 1B). In contrast, marked neointimal formation was observed at 7 days after the injury in M-CSF–treated mice. Quantitative analysis revealed that the I/M ratio in the M-CSF–treated mice significantly increased at 7 days after the injury as compared with that in the control mice (Figure 1C, $P<0.05$); however, there was no difference between the I/M ratio of the control and M-CSF–treated mice at 21 days after the injury (Figure 1D).

Because the histology of neointimal formation at 7 days in M-CSF–treated mice appears to be different from that at 21 days, we performed an immunohistochemical analysis for

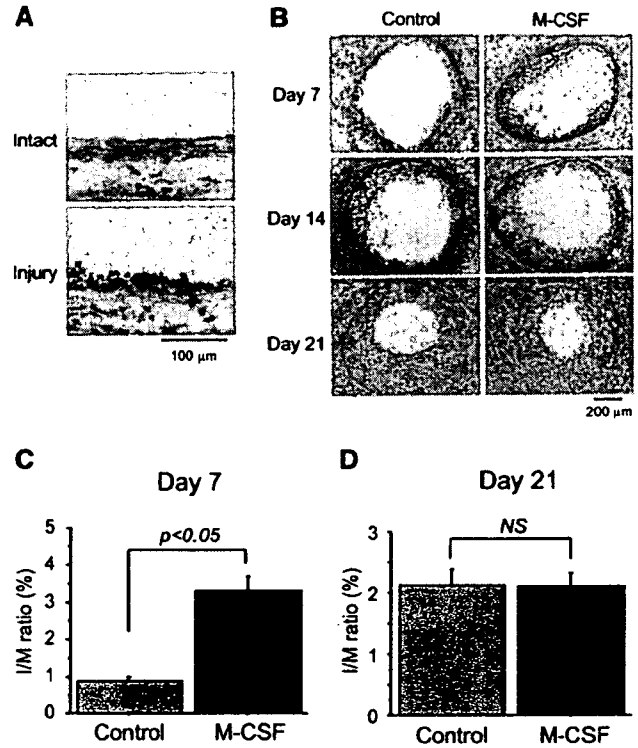

Figure 1. Effect of M-CSF on neointimal formation after vascular injury. A, The injured and uninjured (intact) femoral arteries were excised at 7 days after injury. Immunohistochemical analysis for M-CSF was performed. B through D, M-CSF [500 μg/(kg·day), n=15] or saline (control, n=16) was administered for 10 consecutive days, starting 4 days before the vascular injury. The femoral arteries were excised at 7, 14, and 21 days after the injury. The sample sections were stained with HE, and neointimal formation was evaluated. B, Representative photographs of HE staining. C and D, Bar graphs show the I/M ratio quantified by NIH Image. Data are mean±SEM (each n=5 to 8).

macrophages (F4/80), endothelial cells (CD31), and SMCs (α-SMA). As shown in Figure 2A, endothelial cells on the surface of the lesion and macrophages and SMCs in the lesion were observed. This finding was consistent with the histological features of the lesion at 21 days after injury (data not shown). Next, we assessed whether M-CSF treatment affected reendothelialization at 4 and 7 days after injury and found that M-CSF treatment had no effect (Figure 2B). These results indicate that M-CSF treatment accelerated neointimal formation but not reendothelialization after vascular injury. We further observed the expression of M-CSF receptor, c-fms, in the neointimal lesion of the injured arteries (Figure 2C).

Contribution of Bone Marrow–Derived Cells

To determine the contribution of bone marrow–derived cells to accelerated neointimal formation after vascular injury, we used bone marrow–transplanted mice whose bone marrow was replaced with that of ROSA26 mice. In control mice, almost no β-galactosidase–positive cells were detected, whereas a large number of β-galactosidase–positive cells were detected in M-CSF–treated mice (Figure 3A). These findings suggest that the accelerated neointimal lesion induced by M-CSF mainly consisted of bone marrow–derived cells.

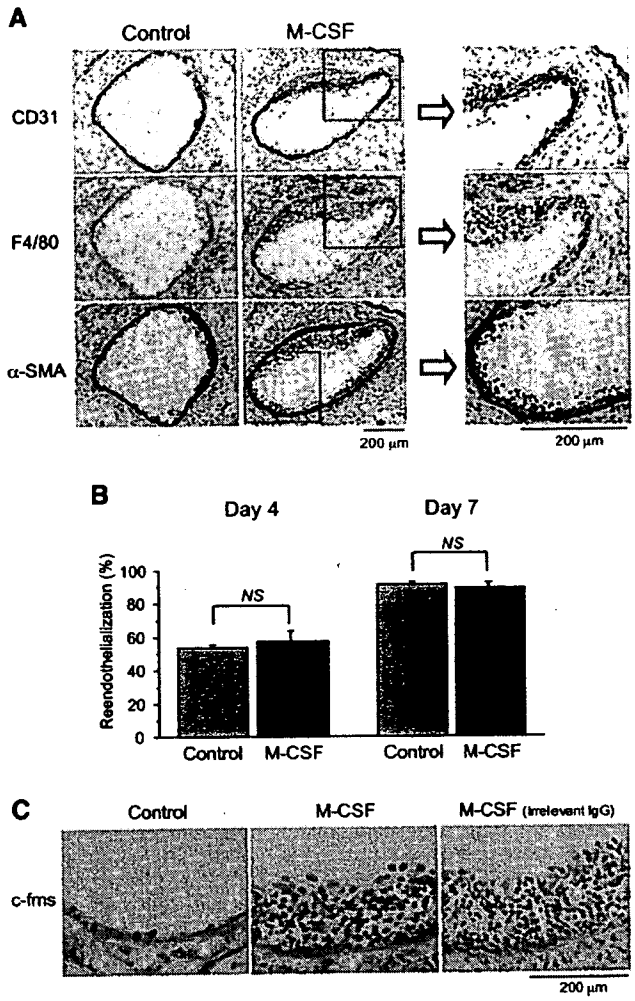

Figure 2. Immunohistochemical staining for endothelial cells, macrophages, and smooth muscle cells. M-CSF [500 μg/(kg·day)] or saline (control) was administered for 10 consecutive days, starting 4 days before the vascular injury. The femoral arteries were excised at 7 days after the injury. Immunohistochemical staining for endothelial cells (CD31), macrophages (F4/80), and SMCs (α-SMA) was performed. A, Representative photographs of CD31, F4/80, and α-SMA expression. B, Bar graphs show the reendothelialization ratio determined by CD31 expression at 4 and 7 days after injury quantified by NIH Image. Data are mean±SEM (n=3 to 4). C, Immunohistochemical staining for c-fms was performed. Irrelevant IgG was used as a negative control.

To explore the types of bone marrow–derived cells that were recruited in the neointimal lesion, we assessed the number of Mac-1$^+$/Gr-1$^-$ (monocytes/macrophages), CD34$^+$/Flk-1$^-$ (EPCs),[13] CD34$^-$/CD14$^+$, and CXCR4$^+$ cells in the peripheral circulation in the control and M-CSF–treated mice. Flow cytometry analysis revealed that M-CSF treatment significantly increased the number of Mac-1$^+$/Gr-1$^-$ cells ($P<0.05$), but not CD34$^+$/Flk-1$^+$ and CD34$^-$/CD14$^+$ cells (Figure 3B though 3D). Interestingly, the number of CXCR4$^+$ cells was also significantly increased by M-CSF treatment. (Figure 3E, $P<0.05$). Further, double staining for Mac-1 and CXCR4 showed that M-CSF-increased peripheral CXCR4$^+$ cells contained Mac-1$^+$ cells (Figure 3F).

Further, at 21 days after injury, we evaluated the contribution of the bone marrow–derived cells to neointimal formation by using bone marrow–transplanted mice whose bone marrow had been replaced with that of GFP mice. Because it was difficult to discriminate GFP-expressing cells from other types of cells in the presence of autofluorescence of the injured artery,[12] we identified the bone marrow–derived cells by immunohistochemical analysis using the anti-GFP antibody. Consistent with the report by Tanaka et al,[14] a considerable number of GFP$^+$ cells were detected in the neointima and media after the injury (supplemental Figure I). Many GFP$^+$ cells in the neointima of the injured artery were positive for the staining against macrophages and SMCs. However, a small number of CD31-positive endothelial cells on the luminal surface of the artery were GFP-positive.

Expression of SDF-1 and CXCR4

Because SDF-1 is a ligand for CXCR4, we performed immunohistochemical analysis to detect SDF-1 in the injured arteries. As shown in Figure 4A, no SDF-1 expression was observed in uninjured arteries, whereas striking SDF-1 expression was observed in the injured arteries of the control and M-CSF–treated mice. Quantitative analysis showed that there was no significant difference in SDF-1 expression levels between control and M-CSF–treated mice (Figure 4B). Further, double immunofluorescence staining showed that SDF-1 was mainly expressed in the neointima and media, whereas CXCR4 was mainly expressed in the neointima (Figure 4C).

Effect of CXCR4 Antagonist on Neointimal Formation

To explore the role of the SDF-1–CXCR4 system, we used a CXCR4 antagonist, AMD3100. AMD3100 [300 μg/(kg·hour)] was subcutaneously administered for 7 days after the vascular injury using a micro-osmotic pump. Consistent with previous reports,[15] the administration of AMD3100 significantly increased the number of circulating white blood cells (WBCs), particularly, neutrophils and lymphocytes, as compared with M-CSF treatment alone (Figure 5A through 5C, $P<0.05$). Additionally, M-CSF treatment markedly increased the I/M ratio at 7 days after the injury (Figure 5D and 5E, $P<0.01$). AMD3100 treatment significantly reduced the increase in the I/M ratio that was caused by M-CSF treatment ($P<0.05$). Immunohistochemical analysis revealed that the number of CXCR4$^+$ cells obviously decreased in the neointima of the AMD3100-treated mice (Figure 5D), but there was no significant difference of the reendothelialization after injury (Figure 5F).

Effect of M-CSF on CXCR4 Expression In Vitro

To investigate the mechanism by which M-CSF increases the number of CXCR4$^+$ cells in peripheral circulation, peripheral and bone marrow MNCs were incubated for 24 hours in the presence or absence of M-CSF, and then analyzed for the expression of Mac-1 and CXCR4. M-CSF treatment significantly increased Mac-1$^+$ cells in peripheral MNCs (Figure 6A, $P<0.05$). However, M-CSF showed no effect on the CXCR4$^+$ cells in the peripheral or bone marrow MNCs, although G-CSF decreased CXCR4$^+$ cells in bone marrow MNCs (Figure 6B though 6D).

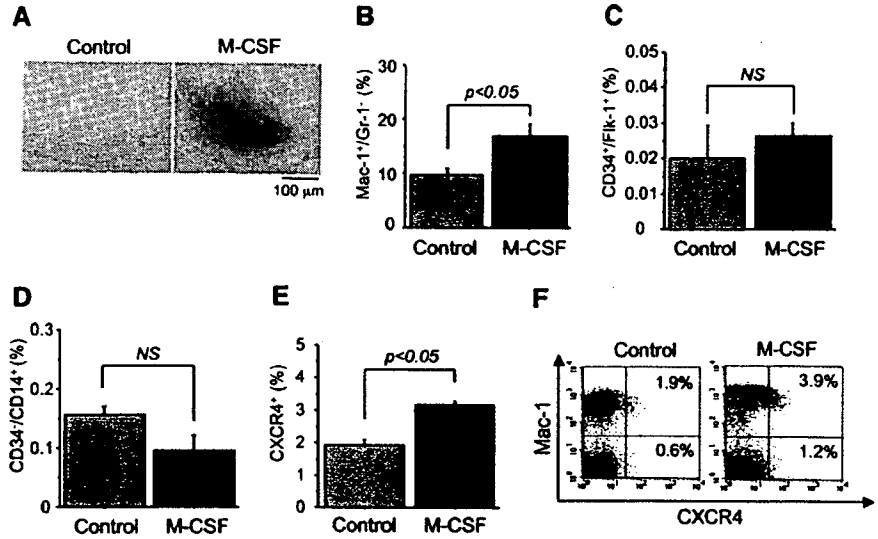

Figure 3. Contribution of bone marrow–derived cells in the early phase. A, Bone marrow–transplanted mice (ROSA26→C57BL/6) were developed, and wire-mediated vascular injury was produced 8 weeks after bone marrow transplantation. M-CSF [500 μg/(kg·day), n=10] or saline (control, n=10) was administered for 10 consecutive days, starting 4 days before vascular injury. The femoral arteries were excised 7 days after the injury, and X-gal staining was performed. B through D, The percentage of $Mac\text{-}1^+/Gr\text{-}1^-$ (B), $CD34^+/Flk\text{-}1^+$ (C), $CD34^-/CD14^+$ (D), and $CXCR4^+$ (E) cells was assessed by using flow cytometry after saline (control) or M-CSF [500 μg/(kg·day)] was administered for 4 consecutive days. Data are mean±SEM (each, n=5). E, Double staining for $Mac\text{-}1^+$ and $CXCR4^+$ cells was performed.

Involvement of Inflammatory Cytokines

Because the inhibition of CXCR4 signaling partially attenuated the accelerated neointimal formation by M-CSF, we investigated whether inflammatory cytokines, such as MCP-1, interleukin (IL)-12p70, IL-10, IL-6, and tumor necrosis factor (TNF)-α, are involved in this process. M-CSF treatment significantly increased the serum of MCP-1 levels ($P<0.05$), but not that of other inflammatory cytokines (supplemental Figure II).

Discussion

The major findings of this study are: (1) M-CSF treatment accelerated neointimal formation in the early phase of vascular injury; this neointimal lesion mainly consisted of bone marrow–derived cells. (2) M-CSF treatment had no effect on EPC mobilization after the injury and reendothelialization of the injured artery. (3) M-CSF treatment increased the number of peripheral $CXCR4^+$ cells; this increase was possibly attributable to the mobilization of $CXCR4^+$ cells from the bone marrow. (4) SDF-1 expression markedly increased in the neointima and media after the vascular injury; a number of $CXCR4^+$ cells were observed in the neointima. (5) A CXCR4 antagonist, AMD3100 significantly attenuated neointimal formation in the early phase after vascular injury in M-CSF–treated mice. These findings suggest that M-CSF treatment accelerates neointima formation in the early phase after vascular injury via the SDF-1–CXCR4 system.

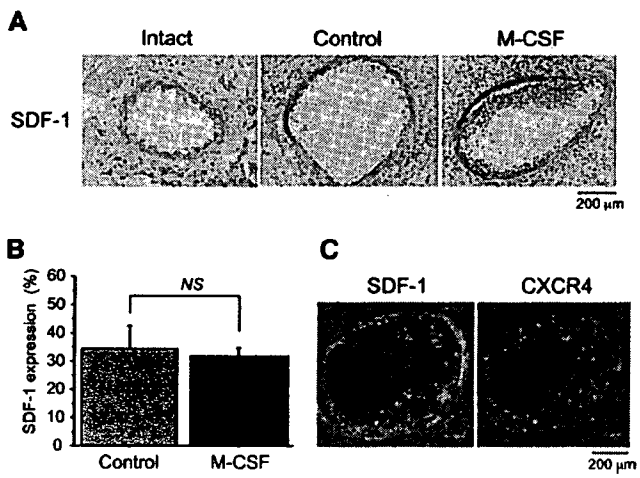

Figure 4. Expression of SDF-1 and CXCR4. M-CSF [500 μg/(kg·day), n=7] or saline (control, n=7) was administered for 10 consecutive days, starting 4 days before vascular injury. The injured and uninjured (intact) femoral arteries were excised at 7 days after injury. A, Immunohistochemical analysis for SDF-1 was performed. B, Bar graph shows the SDF-1 expression quantified by NIH image. Data are mean±SEM (each, n=3 to 4). C, Double immunofluorescence staining for SDF-1 (green) and CXCR4 (red) was performed.

Increasing evidence indicates the importance of vascular progenitor cells derived from the bone marrow in vascular development, homeostasis, and remodeling. In particular, the bone marrow–derived EPCs could promote early reendothelialization of the denuded vessels after injury and potentiate their vascular repair[16]; this suggests the therapeutic potential of EPC transplantation for the treatment of cardiovascular diseases. Because colony-stimulating factors could mobilize bone marrow stem cells into the peripheral circulation, granulocyte CSF (G-CSF) and granulocyte-macrophage CSF (GM-CSF) have been recently noted as clinical application of stem cell therapy.[17,18] However, the effect of M-CSF on vascular repair has not been investigated. Here, we showed that exogenous M-CSF treatment significantly accelerated neointimal formation in the early phase after vascular injury.

In the present study, we used a wire-mediated vascular injury model because this model allows us to reproduce complete endothelial cell denudation and neointimal formation after injury.[12,19] This model induces the robust neointimal formation at 21 days after injury even in the control mice; this suggests that neointimal formation in the control mice could catch up with that in M-CSF–treated mice, and the lesion size in the late phase was similar between the control and M-CSF–treated mice. Xu et al[20] recently showed the importance of M-CSF–c-fms system in the vascular remodeling in a murine cuff-replacement model. We also detected c-fms–positive cells were accumulated in the M-CSF–induced neointimal lesion, indicating the role of M-CSF–c-fms system in the process of neointimal formation after

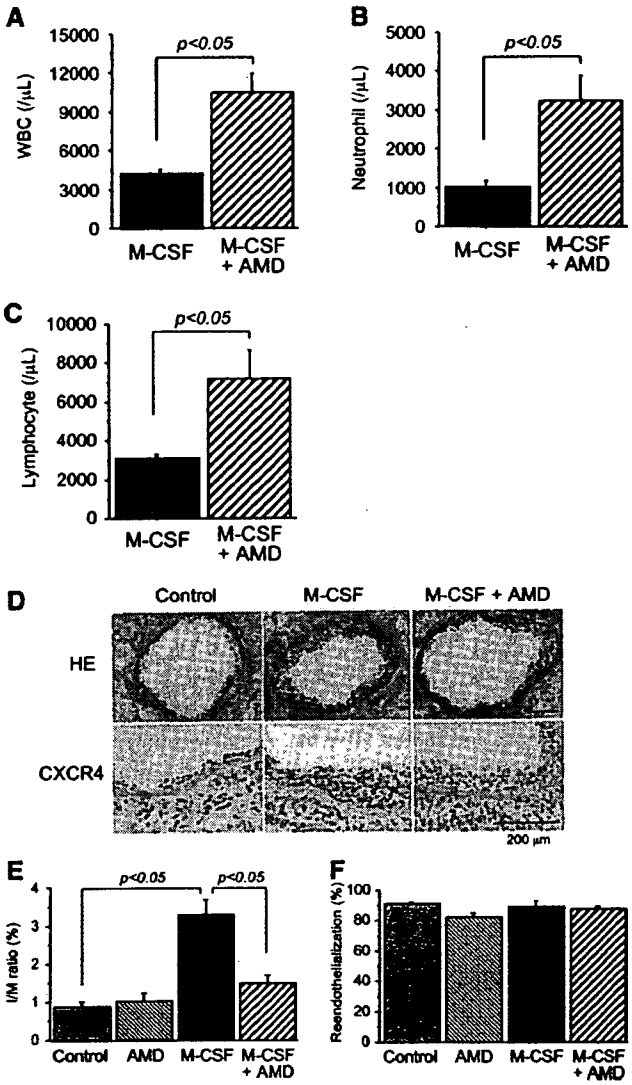

Figure 5. Effect of AMD3100 on neointimal formation. M-CSF [500 μg/(kg·day), n=7] or saline (control, n=7) was administered for 10 consecutive days, starting 4 days before vascular injury. AMD3100 [300 μg/(kg·hour): AMD alone and M-CSF+AMD, each n=7] was administered using a micro-osmotic pump for 7 days after the injury. Blood samples were collected and the femoral arteries were excised at 7 days after the injury. The sample sections were stained with HE and neointimal formation was evaluated. Immunohistochemical analysis for CXCR4 was also performed. A through C, Bar graph shows the number of peripheral WBCs (A), neutrophils (B), and lymphocytes (C). Data are mean±SEM (n=7). D, Representative photographs of HE and CXCR4 staining. E and F, The bar graphs show the I/M ratio (E) and reendothelialization (F), which were quantified by NIH Image. Data are mean±SEM (n=7).

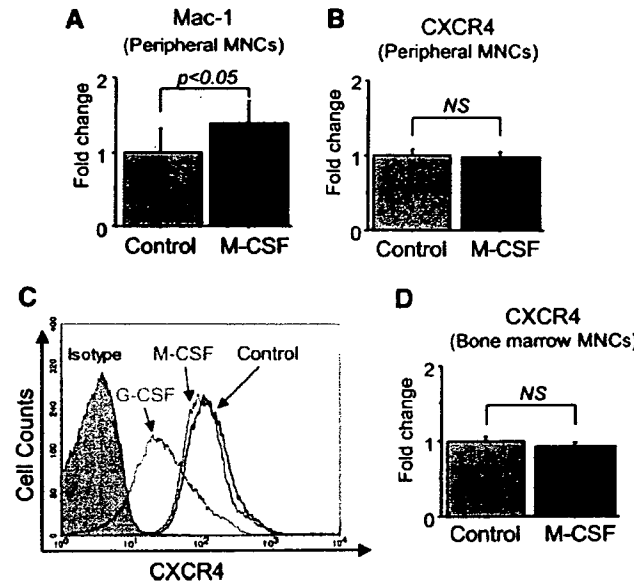

Figure 6. Effect of M-CSF on CXCR4 expression in vitro. Peripheral or bone marrow MNCs were incubated for 24 hours in the presence or absence of M-CSF (100 ng/mL) or G-CSF (100 ng/mL), and then the expression levels of Mac-1 and CXCR4 were analyzed by flow cytometry. Bar graphs show the fold change in the number of Mac-1$^+$ cells in peripheral MNCs (A), CXCR4$^+$ cells in peripheral MNCs (B), and CXCR4$^+$ cells in bone marrow MNCs (D). Data are mean±SEM (each, n=8 to 10). C, Representative histogram of CXCR4 expression in bone marrow MNCs.

injury. Interestingly, Tanaka et al[14] demonstrated that the contribution of bone marrow cells to neointimal formation markedly differs between wire-mediated vascular injury and cuff-replacement models, and suggest that the wire-mediated vascular injury is suitable to investigate the role of bone marrow cells in the vascular remodeling after injury.

We demonstrated that M-CSF had no effect on the mobilization of EPCs, and reendothelialization after vascular injury. Although Harraz et al[2] reported that CD34$^-$ angioblasts were a subset of CD14$^+$ monocytic cells and that these monocytes have the potential to transdifferentiate into endothelial cells, we could not detect increase of peripheral CD34$^-$/CD14$^+$ cells by M-CSF treatment. Recently, Minamino et al[21] showed that M-CSF increased Sca-1$^+$/Lin$^-$, Flk-1$^+$/CD45$^-$, and Sca-1$^+$/c-kit$^+$/CD45$^-$ cells as EPCs in the peripheral circulation. Further studies are needed to clarify the involvement of monocytic cell-derived EPCs in the accelerated neointimal formation by the treatment with M-CSF.

We clearly showed that M-CSF increased the number of CXCR4$^+$ cells in peripheral circulation, whereas the vascular injury induced SDF-1 expression in the injured artery. In this regard, a recent study identified G-CSF downregulation of CXCR4 expression as a mechanism for mobilization of bone marrow myeloid cells.[22] We showed that G-CSF clearly reduced CXCR4 expression in bone marrow–derived MNCs whereas M-CSF had no effect; this suggests that G-CSF and M-CSF may mobilize CXCR4$^+$ cells by distinct mechanisms. The mobilized CXCR4$^+$ cells were recruited; they interacted with SDF-1 and contribute to accelerated neointimal formation, indicating that the SDF-1–CXCR4 system plays an important role in neointimal formation after vascular injury. Although Weber and colleagues[23,24] recently reported that the SDF-1–CXCR4 system contributed to the recruitment of bone marrow–derived SMC progenitor cells and neointimal formation after vascular injury in apoE$^{-/-}$ mice, we could not detect the mobilization of CXCR4$^+$ cells after vascular injury in wild-type mice (data not shown). Therefore, it is possible that SDF-1–CXCR4 system may play a role in vascular repair under specific conditions such as hypercholesterolemia and

M-CSF treatment. More recently, Zhang et al[25] also demonstrated that the SDF-1–CXCR4 system contributed to neointimal formation after carotid artery ligation in endothelial nitric oxide synthase (eNOS) deficient mice. Thus, these investigations strongly support the findings of our study. We showed that although $CXCR4^+$ cells were recruited, M-CSF treatment had no effect on reendothelialization after vascular injury. Additionally, this finding was supported by Weber et al[24] who reported that the neutralization of SDF-1 did not alter the reendothelialization after vascular injury in $apoE^{-/-}$ mice. Conversely, Walter et al[26] reported that the bone marrow MNCs or EPCs of heterozygous $CXCR4^{+/-}$ mice displayed reduced CXCR4 expression and attenuated neovascularization capacity, suggesting that the $CXCR4^+$ cells function as EPCs in ischemic tissue. Taken together, we postulate that the $CXCR4^+$ cells have the potential to function as both EPCs and SMC progenitor cells according to the circumstances, and the SDF-1–CXCR4 system may contribute to the pathogenesis of cardiovascular diseases.

The present study showed that M-CSF treatment increased the level of MCP-1 in serum. Because MCP-1 is a major chemokine that induces the recruitment and activation of monocytes,[27,28] the accumulation of monocytes/macrophages at the injured artery might be mediated, at least in part, via MCP-1 induction.

Treatment with AMD3100 attenuated the M-CSF–induced neointimal formation after vascular injury; this suggests a therapeutic potential of this compound in treating the development of atherosclerosis and restenosis after PCI. Interestingly, recent investigations demonstrated that AMD3100 treatment rapidly mobilizes $CD34^+$ hematopoietic stem cells from the bone marrow into peripheral circulation and synergistically enhances the mobilization of $CD34^+$ cells in combination with G-CSF.[29–31] More recently, Capoccia et al[32] reported that G-CSF combined with AMD3100 promoted angiogenesis in a murine model of hindlimb ischemia. In our study, however, the reendothelialization was not affected by AMD3100. This discrepancy might be attributable to continuous or transient inhibition of CXCR4 signaling. In the study by Capoccia et al,[32] AMD3100 was given by a single injection, while AMD3100 was given by a continuous infusion using an osmotic pump in our study. Therefore, we postulate that continuous CXCR4 inhibition abrogates the chemotactic activity for SDF-1 and homing to the site of vascular injury. Supporting this, a recent study demonstrated that continuous inhibition of CXCR4 signaling impaired functional capacity of EPCs and inhibited angiogenesis.[26] Further investigations are required to use clinical application of this compound.

In summary, we demonstrated that M-CSF mobilized $CXCR4^+$ cells from the bone marrow into peripheral circulation, and vascular injury induced SDF-1 expression in the injured artery. The bone marrow–derived $CXCR4^+$ cells were recruited to the site of the injured artery where they interacted with SDF-1 resulting in the early development of neointimal formation. Further, we showed that the CXCR4 antagonist, AMD3100 significantly inhibited M-CSF–induced neointimal formation. These findings suggest that M-CSF accelerated neointimal formation after vascular injury, at least in part, via the SDF-1–CXCR4 system, and that the inhibition of the SDF-1–CXCR4 pathway might have therapeutic potential in the treatment of vascular injury.

Acknowledgments

We thank Junko Nakayama, Tomoko Hamaji, and Kazuko Misawa for excellent technical assistance, Muneo Yamada (Morinaga Milk Industry Co Ltd) for providing M-CSF, and Masaru Okabe (Osaka University) for providing GFP mice.

Sources of Funding

This study was supported by research grants from the Ministry of Education, Culture, Sports, Science, and Technology (to M.T. and U.I.), the Ministry of Health, Labor, and Welfare (to M.T. and U.I.), and Mitsubishi Pharma Research Foundation (to M.T.).

Disclosures

None.

References

1. Schmeisser A, Garlichs CD, Zhang H, Eskafi S, Graffy C, Ludwig J, Strasser RH, Daniel WG. Monocytes coexpress endothelial and macrophagocytic lineage markers and form cord-like structures in Matrigel under angiogenic conditions. *Cardiovasc Res.* 2001;49:671–680.
2. Harraz M, Jiao C, Hanlon HD, Hartley RS, Schatteman GC. CD34- blood-derived human endothelial cell progenitors. *Stem Cells.* 2001;19: 304–312.
3. Rehman J, Li J, Orschell CM, March KL. Peripheral blood "endothelial progenitor cells" are derived from monocyte/macrophages and secrete angiogenic growth factors. *Circulation.* 2003;107:1164–1169.
4. Dimmeler S, Zeiher AM. Vascular repair by circulating endothelial progenitor cells: the missing link in atherosclerosis? *J Mol Med.* 2004;82: 671–677.
5. Motoyoshi K. Biological activities and clinical application of M-CSF. *Int J Hematol.* 1998;67:109–122.
6. Clinton SK, Underwood R, Hayes L, Sherman ML, Kufe DW, Libby P. Macrophage colony-stimulating factor gene expression in vascular cells and in experimental and human atherosclerosis. *Am J Pathol.* 1992;140: 301–316.
7. Rosenfeld ME, Yla-Herttuala S, Lipton BA, Ord VA, Witztum JL, Steinberg D. Macrophage colony-stimulating factor mRNA and protein in atherosclerotic lesions of rabbits and humans. *Am J Pathol.* 1992;140: 291–300.
8. Qiao JH, Tripathi J, Mishra NK, Cai Y, Tripathi S, Wang XP, Imes S, Fishbein MC, Clinton SK, Libby P, Lusis AJ, Rajavashisth TB. Role of macrophage colony-stimulating factor in atherosclerosis: studies of osteopetrotic mice. *Am J Pathol.* 1997;150:1687–1699.
9. Smith JD, Trogan E, Ginsberg M, Grigaux C, Tian J, Miyata M. Decreased atherosclerosis in mice deficient in both macrophage colony-stimulating factor (op) and apolipoprotein E. *Proc Natl Acad Sci U S A.* 1995;92:8264–8268.
10. Finkelstein A, Makkar R, Doherty TM, Vegesna VR, Tripathi P, Liu M, Bergman J, Fishbein M, Hausleiter J, Takizawa K, Rukshin V, Shah PK, Rajavashisth TB. Increased expression of macrophage colony-stimulating factor after coronary artery balloon injury is inhibited by intracoronary brachytherapy. *Circulation.* 2002;105:2411–2415.
11. Hojo Y, Ikeda U, Katsuki T, Mizuno O, Fukazawa H, Fujikawa H, Shimada K. Chemokine expression in coronary circulation after coronary angioplasty as a prognostic factor for restenosis. *Atherosclerosis.* 2001; 156:165–170.
12. Yoshioka T, Takahashi M, Shiba Y, Suzuki C, Morimoto H, Izawa A, Ise H, Ikeda U. Granulocyte colony-stimulating factor (G-CSF) accelerates reendothelialization and reduces neointimal formation after vascular injury in mice. *Cardiovasc Res.* 2006;70:61–69.
13. Sata M, Nagai R. Inflammation, angiogenesis, and endothelial progenitor cells: how do endothelial progenitor cells find their place? *J Mol Cell Cardiol.* 2004;36:459–463.
14. Tanaka K, Sata M, Hirata Y, Nagai R. Diverse contribution of bone marrow cells to neointimal hyperplasia after mechanical vascular injuries. *Circ Res.* 2003;93:783–790.
15. Martin C, Burdon PC, Bridger G, Gutierrez-Ramos JC, Williams TJ, Rankin SM. Chemokines acting via CXCR2 and CXCR4 control the

release of neutrophils from the bone marrow and their return following senescence. *Immunity*. 2003;19:583–593.
16. Gulati R, Jevremovic D, Peterson TE, Witt TA, Kleppe LS, Mueske CS, Lerman A, Vile RG, Simari RD. Autologous culture-modified mononuclear cells confer vascular protection after arterial injury. *Circulation*. 2003;108:1520–1526.
17. Zohlnhofer D, Ott I, Mehilli J, Schomig K, Michalk F, Ibrahim T, Meisetschlager G, von Wedel J, Bollwein H, Seyfarth M, Dirschinger J, Schmitt C, Schwaiger M, Kastrati A, Schomig A. Stem cell mobilization by granulocyte colony-stimulating factor in patients with acute myocardial infarction: a randomized controlled trial. *J Am Med Assoc*. 2006;295:1003–1010.
18. Deng Z, Yang C, Deng H, Yang A, Geng T, Chen X, Ma A, Liu Z Effects of GM-CSF on the stem cells mobilization and plasma C-reactive protein levels in patients with acute myocardial infarction. *Int J Cardiol*. 2006.
19. Sata M, Maejima Y, Adachi F, Fukino K, Saiura A, Sugiura S, Aoyagi T, Imai Y, Kurihara H, Kimura K, Omata M, Makuuchi M, Hirata Y, Nagai R. A mouse model of vascular injury that induces rapid onset of medial cell apoptosis followed by reproducible neointimal hyperplasia. *J Mol Cell Cardiol*. 2000;32:2097–2104.
20. Xu Y, Arai H, Zhuge X, Sano H, Murayama T, Yoshimoto M, Heike T, Nakahata T, Nishikawa S, Kita T, Yokode M. Role of bone marrow-derived progenitor cells in cuff-induced vascular injury in mice. *Arterioscler Thromb Vasc Biol*. 2004;24:477–482.
21. Minamino K, Adachi Y, Okigaki M, Ito H, Togawa Y, Fujita K, Tomita M, Suzuki Y, Zhang Y, Iwasaki M, Nakano K, Koike Y, Matsubara H, Iwasaka T, Matsumura M, Ikehara S. Macrophage colony-stimulating factor (M-CSF), as well as granulocyte colony-stimulating factor (G-CSF), accelerates neovascularization. *Stem Cells*. 2005;23:347–354.
22. Kim HK, De La Luz Sierra M, Williams CK, Gulino AV, Tosato G. G-CSF down-regulation of CXCR4 expression identified as a mechanism for mobilization of myeloid cells. *Blood*. 2006;108:812–820.
23. Schober A, Knarren S, Lietz M, Lin EA, Weber C. Crucial role of stromal cell-derived factor-1alpha in neointima formation after vascular injury in apolipoprotein E-deficient mice. *Circulation*. 2003;108:2491–2497.
24. Zernecke A, Schober A, Bot I, von Hundelshausen P, Liehn EA, Mopps B, Mericskay M, Gierschik P, Biessen EA, Weber C. SDF-1alpha/CXCR4 axis is instrumental in neointimal hyperplasia and recruitment of smooth muscle progenitor cells. *Circ Res*. 2005;96:784–791.
25. Zhang LN, Wilson DW, da Cunha V, Sullivan ME, Vergona R, Rutledge JC, Wang YX. Endothelial NO synthase deficiency promotes smooth muscle progenitor cells in association with upregulation of stromal cell-derived factor-1alpha in a mouse model of carotid artery ligation. *Arterioscler Thromb Vasc Biol*. 2006;26:765–772.
26. Walter DH, Haendeler J, Reinhold J, Rochwalsky U, Seeger F, Honold J, Hoffmann J, Urbich C, Lehmann R, Arenzana-Seisdesdos F, Aicher A, Heeschen C, Fichtlscherer S, Zeiher AM, Dimmeler S. Impaired CXCR4 signaling contributes to the reduced neovascularization capacity of endothelial progenitor cells from patients with coronary artery disease. *Circ Res*. 2005;97:1142–1151.
27. Takahashi M, Masuyama J, Ikeda U, Kitagawa S, Kasahara T, Saito M, Kano S, Shimada K. Suppressive role of endogenous endothelial monocyte chemoattractant protein-1 on monocyte transendothelial migration in vitro. *Arterioscler Thromb Vasc Biol*. 1995;15:629–636.
28. Takahashi M, Masuyama J, Ikeda U, Kasahara T, Kitagawa S, Takahashi Y, Shimada K, Kano S. Induction of monocyte chemoattractant protein-1 synthesis in human monocytes during transendothelial migration in vitro. *Circ Res*. 1995;76:750–757.
29. Liles WC, Broxmeyer HE, Rodger E, Wood B, Hubel K, Cooper S, Hangoc G, Bridger GJ, Henson GW, Calandra G, Dale DC. Mobilization of hematopoietic progenitor cells in healthy volunteers by AMD3100, a CXCR4 antagonist. *Blood*. 2003;102:2728–2730.
30. Broxmeyer HE, Orschell CM, Clapp DW, Hangoc G, Cooper S, Plett PA, Liles WC, Li X, Graham-Evans B, Campbell TB, Calandra G, Bridger G, Dale DC, Srour EF. Rapid mobilization of murine and human hematopoietic stem and progenitor cells with AMD3100, a CXCR4 antagonist. *J Exp Med*. 2005;201:1307–1318.
31. Flomenberg N, Devine SM, Dipersio JF, Liesveld JL, McCarty JM, Rowley SD, Vesole DH, Badel K, Calandra G. The use of AMD3100 plus G-CSF for autologous hematopoietic progenitor cell mobilization is superior to G-CSF alone. *Blood*. 2005;106:1867–1874.
32. Capoccia BJ, Shepherd RM, Link DC G-CSF and AMD3100 mobilize monocytes into the blood that stimulate angiogenesis in vivo through a paracrine mechanism. *Blood*. 2006.